AD ________________

CONTRACT NUMBER DAMD17-93-C-3118

TITLE: Three-Dimensional Structure Determination of Botulinum Toxin

PRINCIPAL INVESTIGATOR: Ray C. Stevens, Ph.D.

CONTRACTING ORGANIZATION: University of California
Berkeley, California 94720-5940

REPORT DATE: May 1997

TYPE OF REPORT: Annual

PREPARED FOR: U.S. Army Medical Research and Materiel Command
Fort Detrick, Maryland 21702-5012

REPORT DOCUMENTATION PAGE

Form Approved
OMB No. 0704-0188

1. AGENCY USE ONLY *(Leave blank)*

2. REPORT DATE
May 1997

3. REPORT TYPE AND DATES COVERED
Annual / Aug 1, 1995 - May 31, 1997

4. TITLE AND SUBTITLE
Three-Dimensional Structure Determination of Botulinum Toxin

5. FUNDING NUMBERS
DAMD17-93-C-3118

6. AUTHOR(S)
Ray C. Stevens, Ph.D.

7. PERFORMING ORGANIZATION NAME(S) AND ADDRESS(ES)
University of California
Berkeley, California 94720-5940

8. PERFORMING ORGANIZATION REPORT NUMBER

9. SPONSORING/MONITORING AGENCY NAME(S) AND ADDRESS(ES)
U.S. Army Medical Research and Materiel Command
Fort Detrick, Maryland 21702-5012

10. SPONSORING/MONITORING AGENCY REPORT NUMBER

11. SUPPLEMENTARY NOTES

12a. DISTRIBUTION / AVAILABILITY STATEMENT
Approved for public release; distribution unlimited

12b. DISTRIBUTION CODE

13. ABSTRACT *(Maximum 200*

The immediate goals of the contract on the structure and function relationship of botulinum neurotoxin are: 1) Determine the three-dimensional structure of botulinum neurotoxin at atomic resolution by x-ray crystallography. 2) Based on the structure of the neurotoxin, understand the toxins mechanism of action.

We have accomplished the first goal of determining the three-dimensional structure of the 150 kD botulinum neurotoxin serotype A. The toxin is Y-shaped, with a very long alpha-helical translocation domain forming the backbone of the structure. The translocation domain is composed almost entirely of helices, 2 of which are 95 Å in length and form a pseudo-coiled coil. The binding domain and catalytic domain are more globular in shape, located at two different ends of the translocation domain. The overall dimensions of the protein are 120 Å x 80 Å x 40 Å. A complete description of the three-dimensional structure is described in the report. Refinement and analysis of the structure are presently in progress.

14. SUBJECT TERMS
x-ray crystallography, 3-D structure, botulinum neurotoxin

15. NUMBER OF PAGES
45

16. PRICE CODE

17. SECURITY CLASSIFICATION OF REPORT	18. SECURITY CLASSIFICATION OF THIS PAGE	19. SECURITY CLASSIFICATION OF ABSTRACT	20. LIMITATION OF ABSTRACT
Unclassified	Unclassified	Unclassified	Unlimited

FOREWORD

Opinions, interpretations, conclusions and recommendations are those of the author and are not necessarily endorsed by the U.S. Army.

____ Where copyrighted material is quoted, permission has been obtained to use such material.

____ Where material from documents designated for limited distribution is quoted, permission has been obtained to use the material.

RS Citations of commercial organizations and trade names in this report do not constitute an official Department of Army endorsement or approval of the products or services of these organizations.

____ In conducting research using animals, the investigator(s) adhered to the "Guide for the Care and Use of Laboratory Animals," prepared by the Committee on Care and use of Laboratory Animals of the Institute of Laboratory Resources, national Research Council (NIH Publication No. 86-23, Revised 1985).

____ For the protection of human subjects, the investigator(s) adhered to policies of applicable Federal Law 45 CFR 46.

____ In conducting research utilizing recombinant DNA technology, the investigator(s) adhered to current guidelines promulgated by the National Institutes of Health.

____ In the conduct of research utilizing recombinant DNA, the investigator(s) adhered to the NIH Guidelines for Research Involving Recombinant DNA Molecules.

RS In the conduct of research involving hazardous organisms, the investigator(s) adhered to the CDC-NIH Guide for Biosafety in Microbiological and Biomedical Laboratories.

PI - Signature 5/15/97 Date

Three-Dimensional Structure Determination of Botulinum Toxin
Contract: DAMD17-93-C-3118

TABLE OF CONTENTS

INTRODUCTION

Nature of Problem

To determine the 3-dimensional structure of botulinum neurotoxins and their isolated domains. Priority of the specifications are determined in consultation with the Contracting Officer's Representative (COR). The following specifications are listed in the contract section C - Statement of Work:

1) Crystallization of the 150 kD holo-botulinum neurotoxin, serotype A, B, E.

2) Determination of the 3-dimensional structure of serotype A.

3) Given the structure of serotype A, the technique of molecular replacement will be used to determine the structure of serotype B and E.

4) Crystallization of Heavy chain neurotoxin serotype A.

5) Determination of the 3-dimensional structure of the isolated heavy chain. Molecular replacement using the structure of the intact holo-neurotoxin if the structure has not changed substantially. If not, isomorphous replacement will be used.

6) Crystallization of Light chain neurotoxin serotype A.

7) Determination of the 3-dimensional structure of the isolated light chain. Molecular replacement using the structure of the intact holo-neurotoxin if the structure has not changed substantially. If not, isomorphous replacement will be used.

8) Similar studies on other serotypes.

Based on the consultation with the COR, priority is to the 3-dimensional crystal structure of the 150 kD holo-botulinum neurotoxin serotype A.

Background of Previous Work

Before funding of the contracted work for the structure determination of botulinum neurotoxin serotype A, we determined crystallization conditions of botulinum neurotoxin serotype A (Stevens et al, *J. Mol. Biol.* **222**, 877 (1991)) and found the most suitable crystal form of serotype A for X-ray analysis are bipyramidal shaped crystals that crystallize in the hexagonal space group $P3_121$ (or $P3_221$) with one monomer per asymmetric unit. The unit cell dimensions are a = b = 170.5 Å, c = 161.7 Å. Native and derivative data sets have been collected in house (Room 405 Stanley Hall) at the University of California, Berkeley using a shared (with 3 other research groups) Rigaku RU-200 rotating anode generator and R-axis Image Plate area detector system.

During the first 2 years of the 3 year contract, we reported that we had worked out the conditions to further purify the protein (isoelectric focusing and aggregation), stabilize the protein (zinc acetate, proteolytic inhibitors, ganglioside), and improve the crystal quality of the neurotoxin protein. We very carefully worked out condition to collect complete, accurate, and non-deteriorating x-ray diffraction data use flash freezing techniques to freeze the protein crystals at -170^{o}C during x-ray irradiation. We collected a large amount of both native (7 sets) and heavy atom derivative data (20 sets) that is used to phase the x-ray diffraction pattern to yield the 3-dimensional structure of the neurotoxin. Data have been collected at the Brookhaven NSLS and Stanford SSRL synchrotron radiation facilities. As a feasibility study, we initiated crystallization trials of serotype B and E and we have obtained single crystals (completion of Contract Goal C2).

Purpose of Present Work

To complete the contracted work on the 3-dimensional structure determination of botulinum neurotoxin and understand the toxins structure, function, and mechanism of action. Specifically we will locate the heavy atom positions of data collected and phase the diffraction pattern to allow us to trace the electron density of the protein molecule.

Methods of Approach

Using the technique of multiple isomorphous replacement, the 3-dimensional structure of botulinum neurotoxin will be solved using diffraction data from native and heavy atom derivative data sets that are collected in house or at synchrotron facilities. The technique requires one to:

1) Bind heavy atoms to derivative the protein crystal and locate the position of the heavy atom using Patterson methods. The derivitized protein crystals must be isomorphous with the native protein crystals (except for the heavy atom itself) for the information to be interpretable.

2) Once the position of the heavy atoms have been located, approximate phases can be calculated to allow one to observe the electron density of the protein molecule. The program MLPHARE from the CCP4 program suite (CCP4, 1979, The SERC (UK)

Collaborative Computing Project No. 4, a Suite of Programs for Protein Crystallography, distributed from Daresbury Laboratory, Warrington, WA4 4AD, UK) will be used to combine and phase heavy atom derivative data. All computations will be conducted on a Silicon Graphics INDIGO graphics workstation.

3) Fitting of electron density will be made on a Silicon Graphics INDIGO graphics workstation using the program O (version 6.1; Alwyn Jones, 1997).

4) Upon completion of fitting the electron density, the experimental model will be refined using the program XPLOR (version 3.851; Brunger, 1997) installed on a Silicon Graphics INDIGO graphics workstation.

An alternative to isomorphous replacement is the method of molecular replacement which depends on the presence of related structures in different crystals. Proteins which are homologous and have closely similar structures are particularly useful. The near identity of the structures implies relations between different structure amplitudes and phases which are helpful in solving phase problems. Serotypes A, B and E are similar as well as dissimilar (pharmacologically similar, antigenically different). Hence, once a structure is obtained for one serotype, the analysis of crystals of other serotypes can be aided by the molecular replacement technique. This is based on the assumption that the overall tertiary structure of all three serotypes are similar. If this is not the case, then a search for heavy atom derivatives will have to be conducted for all three serotypes.

BODY - Experimental Methods

Although botulinum neurotoxin serotype A crystallizes quite easily, the ability to collect x-ray diffraction data on protein crystals that are all "locked" into the same structure inside the crystal has become a hurdle in our efforts to determine the 3-dimensional structure. In layman's terms, botulinum neurotoxin molecules have the ability to conform to several different conformational structures caused by "floppy" or disordered regions of protein structure. This problem makes it difficult to merge together native data sets as well as heavy atom derivative data sets. This problem makes it difficult to use the techniques of isomorphous replacement with heavy atom derivatives since one data set is not similar enough to the next. To avoid this problem we have taken several different measures that are described below. These approaches have proven successful to other researchers that have encountered this problem. The problem of non-isomorphism is not uncommon in crystal structure determinations, particularly for neurotoxins (i.e. crystal structure determinations for cholera toxin, diphtheria toxin, pertussis toxin).

2) Neurotoxin Data Collection (Table I).

Data have been collected on approximately 150 data sets in house with a series of different transition metals, sugar molecules, gangliosides, inhibitors to zinc proteases, different pH conditions, and various salts to resolve the issue of the protein molecules packing in different orientations in the crystal lattice. Each different compound is used to collect data on two different crystals in order to confirm the effects that are observed. The addition of additives is to "lock" the protein molecules into one conformation. This will allow the technique of MIR to be used for the crystal structure determination. Perhaps the most critical step in determining the crystal structure was the change from the crystal form that was being used in previous years (~1.1 M sodium formate, 100 mM Hepes pH 7) to a new crystallization conditions (200 mM Mg acetate and ~10% PEG4K, pH 7). The toxin has been crystallized in 5 different crystal morphologies, all five belonging to the same space group P3121. The common theme of acetate in the buffer and derivative most likely helped with isomorphism.

3) Heavy Atom Derivative Data Collection (Table I).

In addition to the numerous data sets collected in house, we have also collected data at two different synchrotron sources and tuned the wavelength to the absorption edge of the metal that we have bound to the protein. This approach allows us to determine the 3-D structure of the neurotoxin using anomalous dispersion of the heavy atom and maximizing the heavy atom signal. The additional data obtained from the anomalous signal can be enough to determine the crystal structure with a single derivative or at least increase the amount of usable data from one derivative. Of particular use in our study, are acetate based derivatives, since the crystal form finally used in the structure determination was from PEG-400 and Mg acetate mother liquor. Based on prior experiments, 5 free thiol groups are accessible and therefore mercury and gold derivatives are good choices for heavy atom derivatives of the toxin. The samarium and uranium derivatives bind to positively charged pockets. Merging statistics in Table I include all data to the highest resolution bin without throwing away any data.

Table I - X-ray Data collected between March - April, 1997
on Botulinum Neurotoxin serotype A (Crystal space group P3121)

DataSet Name	Resolution Å	Unit Cell (a,c) Å	#Refl. collected	#Refl. unique	Complete %	I/sig	R_{merge} %	$R_{mergetonative}$ %
Synchrotron Radiation Data Collection Trips								
(SSRL March 97)								
Native	3.6	170.8, 161.1	97,575	28,963	91.8 (76.4)	9.0	9.1 (37.3)	-
HgCl	4.5	169.8, 160.9	87,457	15,830	97.2 (96.0)	6.5	12.9 (20.1)	21.7
HgAc	4.2	169.9, 161.2	86,260	19,650	97.8 (94.3)	7.1	9.1 (24.5)	21.0
SmAc	4.5	170.6, 161.0	22,797	12,516	78.5 (78.2)	7.9	7.6 (17.4)	14.9
UrAc	4.5	170.7, 161.1	22,795	11,796	71.9 (73.6)	7.8	9.3 (16.1)	15.2
KAuCl	6.0	170.7, 161.0	19,894	6,080	93.7 (95.5)	10.7	9.6 (26.2)	15.2

Highest resolution statistics are shown in parentheses

Abbrevations for heavy atom derivatives - all soaks were completed at room temperature. All data collected at 4°C.

HgCl	3 mM soak for 6 hours with methyl mercury chloride
HgAc	1mM (saturated) for 6 hours with mercury acetate
SmAc	50 mM for 12 hours with samarium acetate
UrAc	0.5 mM for 6-10 hours with uranyl acetate
KauCl	1 mM for 8-12 hours with potassium gold tetrachloride

4) Location of Heavy Atom Sites for Phasing

Interpretation of Patterson maps to locate the positions of the heavy atoms has been completed, the following heavy atom sites along with the derivative name are listed below. The derivative abbreviations are listed in Table I.

Metal	x	y	z	Occ.	B-factor
HgAc	0.9402	0.8193	0.0162	0.77	20.0
HgAc	0.6051	0.3112	0.0811	0.46	20.0
HgAc	0.0852	0.7199	0.3591	0.48	20.0
HgAc	0.1275	0.0563	0.6916	0.40	20.0
HgAc	0.3610	0.3171	0.3135	0.50	20.0
HgAc	0.2829	0.7060	0.2922	0.42	20.0
SmAc	0.4911	0.8897	0.0603	0.76	20.0
SmAc	0.4374	0.2335	0.4240	0.70	20.0
SmAc	0.0881	0.8896	0.1364	0.43	20.0
UAc	0.4952	0.8924	0.0593	0.55	20.0
UAc	0.4397	0.2367	0.4331	0.38	20.0
UAc	0.4095	0.2901	0.2264	0.35	20.0
AuCl	0.7206	0.4196	0.0368	0.93	20.0
HgCl	0.941	0.820	0.016	0.81	20.0
HgCl	0.364	0.280	0.308	0.64	20.0
HgCl	0.128	0.056	0.694	0.30	20.0
HgCl	0.690	0.294	0.412	0.43	20.0
HgCl	0.954	0.641	0.982	0.54	20.0
HgCl	0.424	0.717	0.963	0.51	20.0

5) Phasing of Diffraction Data from MLPHARE (CCP4 Program Suite). Data were phased with 5 derivatives to 5.0 Å resolution, and the phases were extended to 3.6 Å resolution with the program DM (CCP4 program suite) using the solvent flattening/histogram matching algorithm. Although the mercury derivatives and the gold derivatives have sites in common, the occupancy differences appears to allow them to complement one another, rather than interfere with one another in the phasing statistics.

<4SSQ/LL>	Resol	Nref_a	DISO_a	LOC_a	PhP_a	CullR_a	Nref_c	DISO_c	LOC_c	PhP_c	CullR_c
0.009	10.75	634	252.0	178.0	1.19	0.71	134	350.9	248.6	0.79	0.71
0.014	8.37	1142	229.7	154.5	1.30	0.67	190	325.1	210.7	0.93	0.65
0.021	6.86	1831	181.7	112.4	1.73	0.62	229	243.9	163.3	1.10	0.67
0.030	5.81	2685	153.0	96.5	1.96	0.63	278	228.8	158.8	1.16	0.69
0.039	5.03	1173	160.0	110.3	1.69	0.69	105	202.3	152.2	1.32	0.75
0.051	4.44	0	0.0	0.0	0.00	0.00	0	0.0	0.0	0.00	0.00
0.063	3.98	0	0.0	0.0	0.00	0.00	0	0.0	0.0	0.00	0.00
0.077	3.60	0	0.0	0.0	0.00	0.00	0	0.0	0.0	0.00	0.00
TOTAL		7465	181.3	118.4	1.64	0.65	936	266.6	182.6	1.03	0.68

6) Determination of molecular envelope and protein boundary

Shown in Figure 1 is the unit cell packing of the phased electron density. In black, are the solvent regions between protein molecules. The solvent content is estimated at 67% assuming one molecule per asymmetric unit (6 molecules per unit cell). The unit cell is shown as a box in thin lines. Shown in Figure 2 is the packing of the toxin molecules in the unit cell.

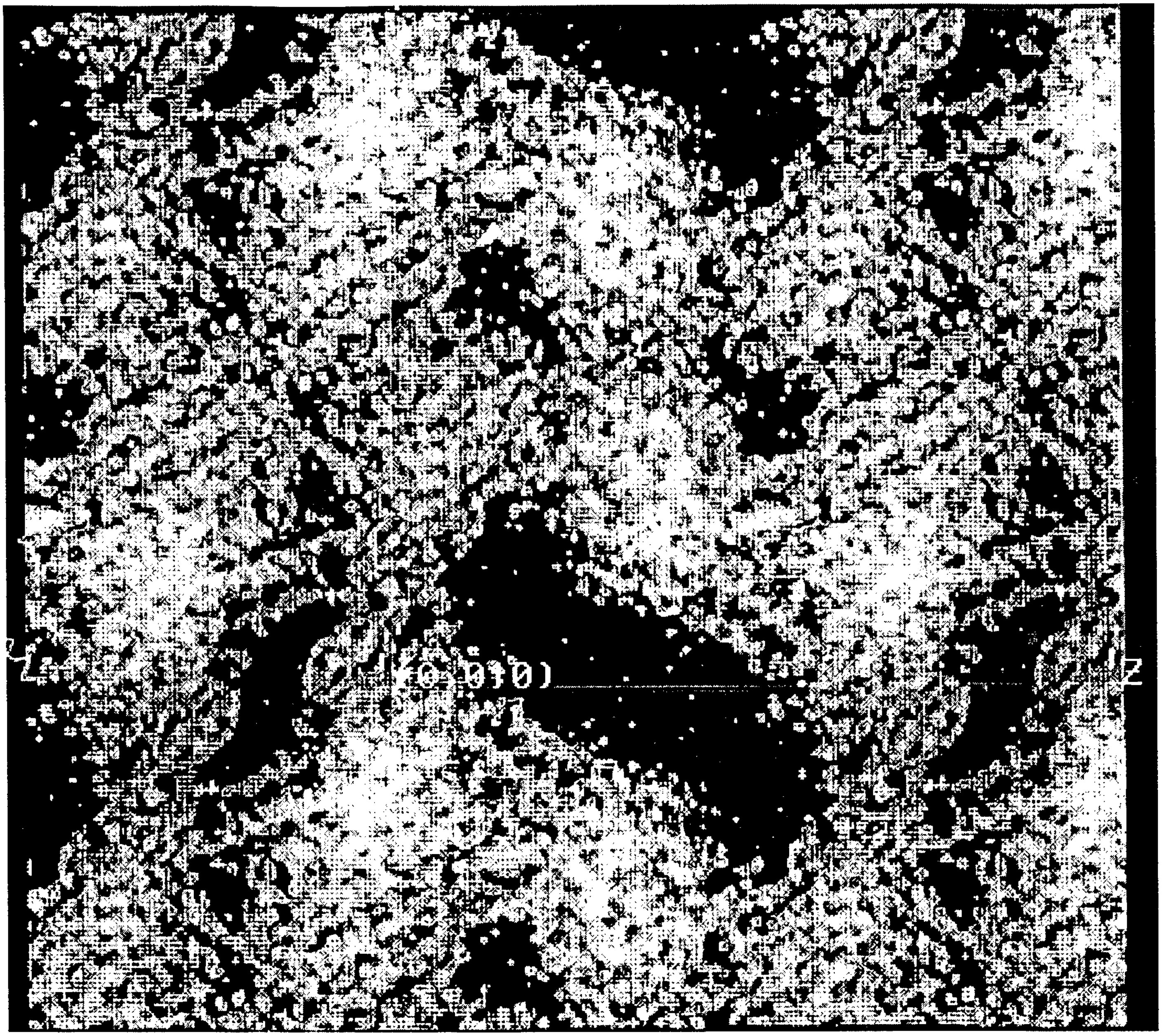

Figure 1.

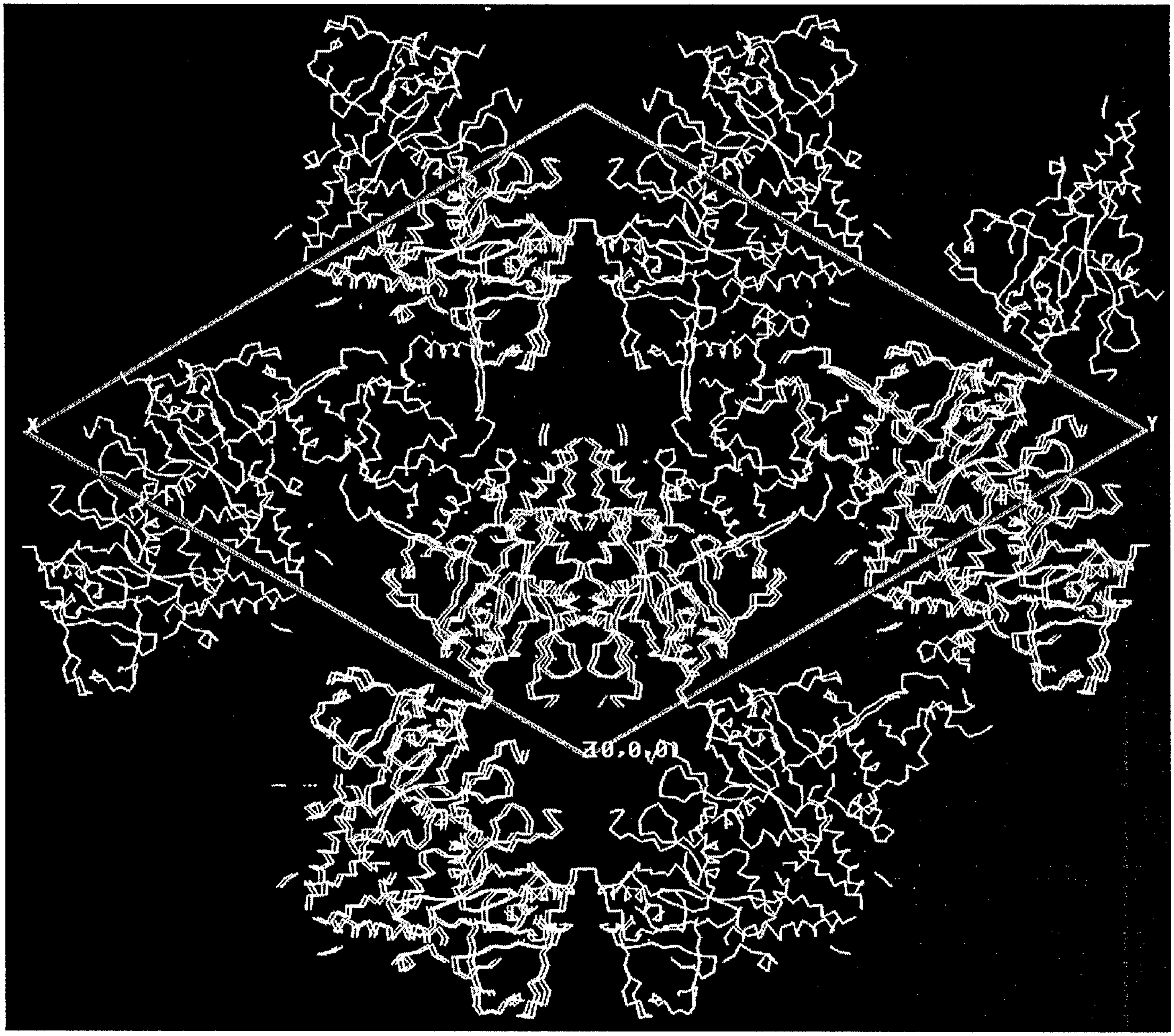

Figure 2

7) Tracing electron density with poly-alanine model

Shown in Figure 3 are two views of the electron density for the long helix observed in the translocation domain. In Figure 4 are two preliminary models of botulinum neurotoxin. Based on the molecular envelope, and using "bones" tracing, a poly-alanine model is placed into the electron density. The program O was used for all model building. Figure 5 illustrates the secondary structure assignment to date for the three domains. The translocation domain is almost all alpha-helix, followed by the catalytic domain in second, and the binding domain having the least amount of secondary structure.

The steps in the model building are as follows:

1) Place poly-alanine secondary elements into electron density, starting with the alpha-helices, and then beta-strands.

2) Determine directionality of the secondary elements (N-terminus versus C-terminus).

3) Connect secondary elements where possible.

4) Assign sequence residue to poly-alanine trace for large side chains (Trp, Tyr, Phe).

5) Complete as much of the trace and sequence assignment as possible.

6) Refine the initial model into the electron density.

7) Perform successive rounds of model building and refinement, until the structure has converged to an acceptable crystallographic R-value and free R-vale.

Electron Density of Botulinum Neurotoxin Translocation Domain 94 A Helix

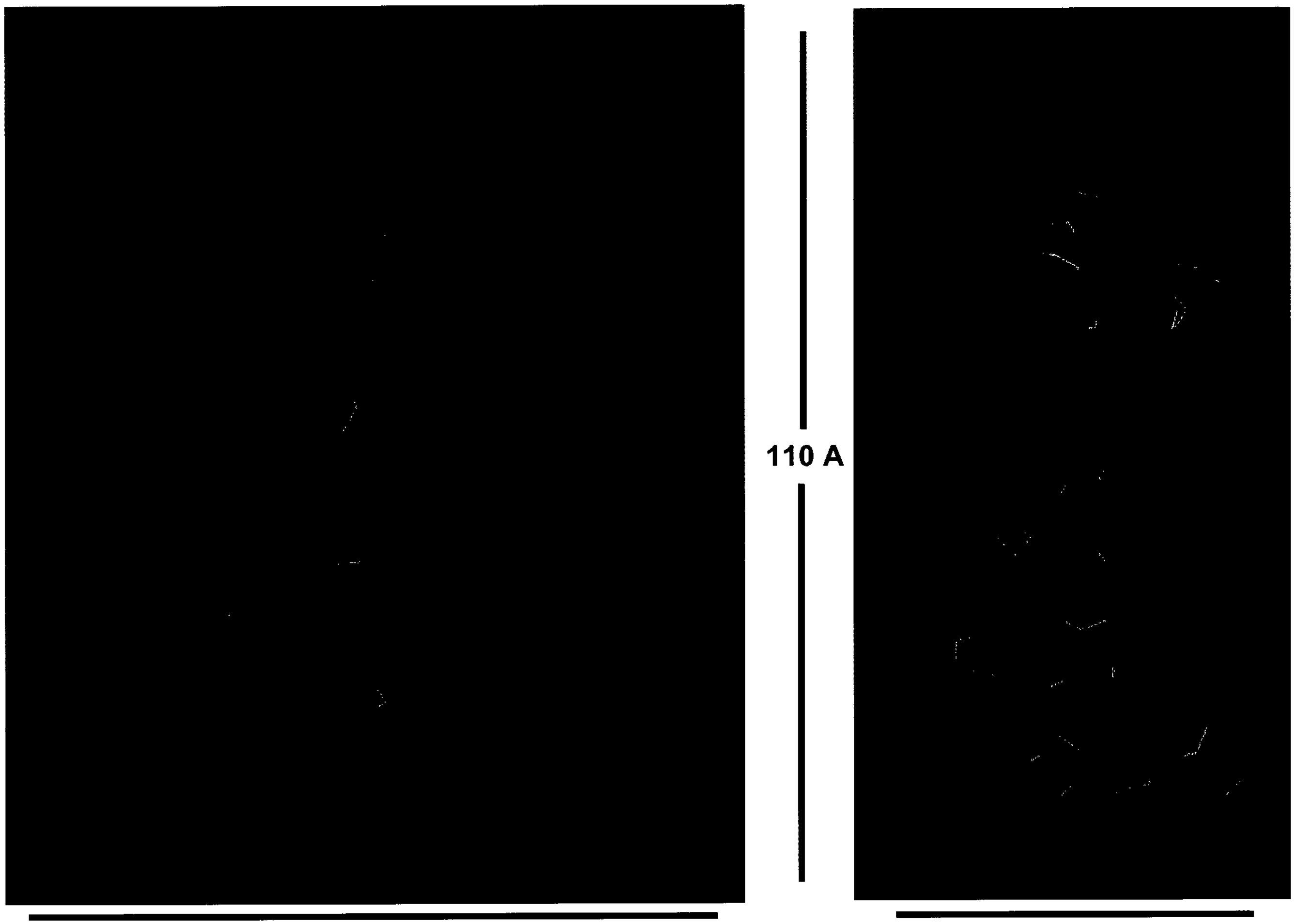

150 kD Botulinum Neurotoxin Crystal Structure

BT Binding Domain

NIINTSILNL RYESNHLIDL SRYASKINIG SKVNFDPIDK NQIQLFNLES SKIEVILKNA

IVYNSMYENF STSFWIRIPK YFNSISLNNE YTIINCMENN SGWKVSLNYG EIIWTLQDTQ

EIKQRVVFKY SQMINISDYI NRWIFVTITN NRLNNSKIYI NGRLIDQKPI SNLGNIHASN

NIMFKLDGCR DTHRYIWIKY FNLFDKELNE KEIKDLYDNQ SNSGILKDFW GDYLQYDKPY

YMLNLYDPNK YVDVNNVGIR GYMYLKGPRG SVMTTNIYLN SSLYRGTKFI IKKYASGNKD

NIVRNNDRVY INVVVKNKEY RLATNASQAG VEKILSALEI PDVGNLSQVV VMKSKNDQGI

S-S S-S

TNKCKMNLQD NNGNDIGFIG FHQFNNIAKL VASNWYNRQI ERSSRTLGCS WEFIPVDDGW

GERPL -- C

Helix

Strand

BT Catalytic Domain

PFVNKQFNYK DPVNGVDIAY IKIPNVGQMQ PVKAFKIHNK IWVIPERDTF TNPEEGDLNP

PPEAKQVPVS YYDSTYLSTD NEKDNYLKGV TKLFERIYST DLGRMLLTSI VRGIPFWGGS

TIDTELKVID TNCINVIQPD GSYRSEELNL VIIGPSADII QFECKSFGHE VLNLTRNGYG

Zn

STQYIRFSPD FTFGFEESLE VDTNPLLGAG KFATDPAVTL AHELIHAGHR LYGIAINPNR

VFKVNTNAYY EMSGLEVSFE ELRTFGGHDA KFIDSLQENE FRLYYYNKFK DIASTLNKAK

SIVGTTASLQ YMKNVFKEKY LLSEDTSGKF SVDKLKFDKL YKMLTEIYTE DNFVKFFKVL

NRKTYLNFDK AVFKINIVPK VNYTIYDGFN LRNTNLAANF NGQNTEINNM NFTKLKNFTG

LFEFYKLLCV RGIITSKTKS LDKGYNK

Helix

Strand

BT Translocation Domain

LC Connection
residue 453

```
      ALN  DLCIKVNNWD  LFFSPSEDNF  TNDLNKGEEI  TSDTNIEAAE  ENISLDLIQQ
YYLTFNFDNE  PENISIENLS  SDIIGQLELM  PNIERFPNGK  KYELDKYTMF  HYLRAQEFEH
GKSRIALTNS  VNEALLNPSR  VYTFFSSDYV  KKVNKATEAA  MFLGWVEQLV  YDFTDETSEV
STTDKIADIT  IIIPYIGPAL  NIGNMLYKDD  FVGALIFSGA  VILLEFIPEI  AIPVLGTFAL
VSYIANKVLT  VQTIDNALSK  RNEKWDEVYK  YIVTNWLAKV  NTQIDLIRKK  MKEALENQAE
ATKAIINYQY  NQYTEEEKNN  INFNIDDLSS  KLNESINKAM  ININKFLNQC  SVSYLMNSMI
PYGVKRLEDF  DASLKDALLK  YIYDNRGTLI  GQVDRLKDKV  NNTLSTDIPF  QLSKYVDNQR
LLSTFTEYIK  NI
```

Helix

Strand

8) Proteolytic Assay of Catalytic Domain

Because of the need for a means to evaluate the quality of protein used in crystal growth experiments in addition to the fact that we need to learn as much as possible about the behavior of the protein during crystal growth experiments and to help us understand the function of the neurotoxin once the structure is determined, we have initiated simple kinetic assays to evaluate the neurotoxins proteolytic activity. The substrate being used is a 17 amino acid peptide of the synaptic vesicle protein SNAP-25. After several months of attempting to optimize proteolytic activity, it was determined that the zinc concentration of the toxin must be 100 micromolar. If the concentration of any zinc salt is above the micromolar range, the neurotoxin activity is inhibited. If the concentration of any zinc salt is below the micromolar range, the neurotoxin activity is very low (less than 10% of full activity). With this information, we now routinely use 100 μM zinc acetate in all crystallization conditions to help stabilize the neurotoxin. It cannot be overemphasized that micromolar concentrations of zinc are absolutely necessary for full activity. In similar zinc protease structures, it is observed that correct concentrations of zinc atoms can possess either structural/catalytic or both roles in aiding the proteolytic activity. In the case of botulinum neurotoxin, we believe zinc to play both roles since we have observed that zinc salts stabilize the crystal growth under the optimal conditions (micromolar).

Analogous to other crystal structure determinations, it has frequently been observed that inhibitors for enzymes aid in the stabilization of protein molecules by locking the enzyme into a single stable conformation. By using the above kinetic assay, we have been able to screen potential inhibitors of the neurotoxin to stabilize a single conformation. The inhibitors being investigated including peptide-like analogs synthesized by Professor Paul Bartlett in the Dept. of Chemistry of UC-Berkeley. Based on the protease recognition site, we are investigating the inhibitors Z-Ala-Gly-P-Phe-, Z-Phe-P-Leu-Ala-, Z-Gly-Ala-P-, and CbZ-Gly-P-Leu-Gly-. The "-P-" moiety is a phosphate backbone in place of the amide backbone that strengthens the peptide bond and does not allow cleavage by the protease. The inhibitor does however have the recognition elements that the neurotoxin binds.

9) Isolated Domains of Botulinum Neurotoxin Serotype A

Recombinant DNA work on serotype A domains to produce protein for crystallography experiments. High expression levels of the translocation domain of BT serotype A have been achieved and purified. The E. coli expressed protein is folded and appears to be composed of both a-helices and beta-sheets based on CD (circular dichroism) experiments conducted in my laboratory. Since the present crystals of botulinum neurotoxin diffract to 3.0 Å resolution, we will be able to determine the 3-dimensional structure of the neurotoxin and observe secondary structure elements (alpha helices, beta strands, and beta sheets). It will be difficult to observe detailed side chain interactions of the smaller side chains (the larger side chains should easily be observable). In order to obtain a more detailed picture of the protein structure, recombinant DNA work on isolated domains (binding, translocation, catalytic) have been initiated with the goal of crystallizing the domains and determining the 3-D structure by x-ray crystallography. The approach of "divide & conquer" has been used in numerous examples to determine the structure of regions of protein molecules (i.e. SH2 & SH3 domains of tyrosine kinases).

All work on this aspect of the project has been conducted by personnel supported by the Department of Chemistry at UC-Berkeley. Proper authorization to conduct recombinant DNA work on fragments of botulinum neurotoxin were obtained from the Biosafety Officer, Office of Environment, Health and Safety (see Annual Report from previous year).

This work is in line with goals C5 and C7 of the contracted work, to crystallize the isolated domains of botulinum neurotoxin. Large quantities of purified protein is required and a recombinant approach is being taken. The alternative approach is by purifying the light and heavy chains from one another. This approach would require twice or greater the amount of holo-neurotoxin plus purification. Secondly, it is impossible to separate the binding domain from the translocation domain in this fashion.

Relationship to Goals of Research

All work to date focuses on the single goal of determining the 3-D structure. Although numerous side projects have emerged (kinetic assay, binding assays, recombinant DNA work), all of these projects are to aid in the crystal structure determination goal. Furthermore, the information obtained during these studies will be mandatory in understanding the function of the neurotoxin once the structure is known. All of the side projects listed above have been completed by personnel not supported by this contract. The individuals supported by the contract work only on the crystal structure determination.

CONCLUSION

We have accomplished the primary objective outlined in the research contract - the three-dimensional structure determination of botulinum neurotoxin serotype A. We have cloned and expressed the isolated domains, and crystallized the translocation domain. We have crystallized two other serotypes of botulinum neurotoxin (serotype B and E). This work has opened the door to a great deal of future work on understanding how the molecule functions. Furthermore, the results open the door for the design of inhibitors for the toxins activity. Already, we can speculate how the translocation domain interacts with the membrane based on h long helices analogous to the helices in influenza virus hemaglutinin.

Future work on this project includes the refinement of the botulinum neurotoxin model, an increase in diffraction resolution for a higher resolution structure, and experiments to deduce the mechanism of action for each of the domains (binding, translocation, catalytic) of botulinum neurotoxin.

BIBLIOGRAPHY

Publications

Manuscript 1 - "Recombinant Expression and Purification of the Botulinum Neurotoxin Type A Translocation Domain" B. Lacy and R.C. Stevens, submitted to *Protein Expression and Purification.*

Manuscript 2 - "Antibody Mapping to Domains of Botulinum Neurotoxin Serotype A in the Complexed and Uncomplexed Forms. Chen et al., *Infection & Immunity*, 65, 1626 (1997).

Meeting Abstracts

"Structural Features of Botulinum Neurotoxin Serotype A toxicity"
2nd International Meeting on the Molecular Genetics and Pathogenesis of the Clostridia, Onzain, France June 22-25, 1997.

Personnel Conducting Research on the Project at Univ. California-Berkeley

Professor Raymond C. Stevens
Dr. Cara Marks
Dr. Hanne Merritt
Heather Manning
Borden Lacy
Alona Cohen

Personel Conducting Research on the project at U. Wisconsin-Madison (sub-contract)

Bibhuti DasGupta
Bill Tepp
Mary Evenson

Recombinant Expression and Purification of the Botulinum Neurotoxin Type A Translocation Domain¶

Running Title: Expression of Botulinum Neurotoxin Translocation Domain

Borden Lacy and Raymond C. Stevens*
Department of Chemistry, University of California, Berkeley, California 94720

* Indicates author to whom correspondence should be addressed.
Phone (510) 643-8285, Fax (510) 643-9290

Appendix A

¶ This work was supported in part by the U. S. Army Medical Research and Development Command (DAMD17-93-C-3118), a NSF predoctoral fellowship (B.L.), and a NSF Young Investigator Award (R.C.S.).

1 The abbreviations used are: BTA, botulinum neurotoxin type A; BT, botulinum neurotoxin; DT, diphtheria toxin; Tris, tris(hydroxymethyl)aminomethane; ECL, enhanced chemiluminescence; IPTG, isopropyl β-D-thiogalactopyranoside; PCR, polymerase chain reaction; EDTA, ethylenediaminetetraacetic acid; BT-trans, botulinum neurotoxin translocation domain; CD, circular dichroism; ELISA, enzyme linked immunosorbent assay; PBS, phosphate buffered saline; scFv, single chain variable fragment; Fc, constant fragment; SDS-PAGE, sodium dodecyl sulfate-polyacrylamide gel electrophoresis; PE, *Pseudomonas* exotoxin A.

ABSTRACT

Botulinum neurotoxin type A in its fully activated form exists as a di-chain protein consisting of a light chain (MW~50-kDa) and heavy chain (MW~100-kDa) linked by a disulfide bond (1). The protein can be further subdivided into three functional domains: a catalytic domain corresponding to the light chain, a translocation domain associated with the N-terminal half of the heavy chain, and a binding domain as the C-terminal half. To facilitate further structural and functional studies on the mechanism of toxin translocation, we report here the recombinant *Escherichia coli* expression and purification of the isolated translocation domain with a yield of 1 mg pure protein per 1 g cell paste. Circular dichroism, enzyme linked immunosorbent assays (ELISA), and preliminary crystallization experiments verify proper protein folding. This reagent should serve as a key tool in elucidating the mechanism of translocation and in determining how the catalytic domain, a large 50-kDa metalloprotease, is delivered to the cytosol.

INTRODUCTION

Botulinum neurotoxin serotype A (BTA)[1] is one of seven antigenically distinct proteins produced from strains of *Clostridium botulinum*. These serotypes (designated types A-G) are the causative agents of botulism, a potentially fatal condition of neuromuscular paralysis (2). The seven types of BT along with tetanus toxin comprise the clostridial toxin family. Comparison of the clostridial toxins to the better characterized diphtheria toxin (DT) shows some important similarities. Both the clostridial toxins and DT are synthesized as a single chain and then post-translationally nicked to form a di-chain molecule held together by a disulfide bond. Their toxicity is believed to be a result of three functional domains (Fig. 1a shows BTA) acting in a three-step mechanism to bind, enter, and catalyze a specific reaction within the cell. The idea that BT shares this three-step model of toxicity was first proposed by Simpson (3) and has since been supplemented with experimental evidence and analogies to DT. The first step involves a binding interaction between the 50-kDa binding domain and a cell surface receptor on the pre-synaptic membrane (4). BT is thought to be internalized into an endosome via receptor-mediated endocytosis. The acidic pH of the endosome is believed to then cause a conformational change (best characterized for DT, (5-6)) in the 50-kDa translocation domain which allows it to interact with the endosomal membrane and form a channel (7-8). The 50-kDa catalytic domain is translocated across the membrane, released from its disulfide linkage, and left free in the cytosol. The catalytic domain of each BT serotype is a zinc-dependent endopeptidase which targets specific sequences of proteins involved in vesicle-docking and membrane fusion. BTA's cleavage of a peptide bond in SNAP-25 (synaptosomal associated protein of 25-kDa) (9) results in inhibition of acetylcholine release from the axon and, ultimately, paralysis (10).

Of particular interest is the proposed role of the BT translocation domain in the delivery of the catalytic domain to the cytosol. Specifically, (i) the nature of the conformational change at acidic pH, (ii) the molecular mechanism of insertion, and (iii) the role the translocation domain plays-- active or passive-- in getting the 50-kDa catalytic domain into the cytosol.

A great deal of insight into the phenomenon of translocation has come from studies done on diphtheria toxin, particularly since the elucidation of the atomic coordinates by x-ray crystallography (11). Using biochemical studies, researchers have used this structural information to assess the roles that both secondary structural elements and individual amino acids play in the translocation event (12-16).

In contrast, very little information about translocation is available for the clostridial toxins. While comparisons between toxin families have been useful in the initial understanding of BT, significant differences exist. Most notably, DT is a 58-kDa protein while BT is 150-kDa. The enormous size of BT relative to DT and all other toxins makes it uniquely interesting, especially in the context of cellular transport. Sequence comparisons indicate that when aligned to BTA, the other serotypes and tetanus toxin have 55 to 66% homology. The translocation domains share a slightly higher homology of 60 to 70%. We, therefore, have pursued BTA as a model system for studying translocation of the clostridial toxins.

As a first step in this investigation, the isolated translocation domain of BTA has been cloned into a recombinant *E. coli* overexpression system. This is the first report of translocation domain expression for botulinum neurotoxin along with initial biophysical characterization. Constructs were prepared both with and without cysteines and with silent mutations to improve homogeneity. Given the partial membrane-protein character of the domain, a detailed description of the purification and folding analysis is presented as well as preliminary structural experiments.

EXPERIMENTAL PROCEDURES

Materials - All buffer components and reagents were purchased from Sigma unless otherwise specified: Tris (Fisher Scientific); Enhanced Chemiluminescence (ECL) reagents (Amersham); DNAse (Boehringer Mannheim); silver staining solutions (BioRad); Isopropyl β-D-thiogalactopyranoside (IPTG) (Diagnostic Chemicals, Inc.). Restriction endonucleases were obtained from New England Biolabs, Inc. and used as directed by the supplier. T4 DNA ligase, T4 polymerase, T4 polynucleotide kinase were obtained from Pharmacia Biotech, Inc. Additionally, Pharmacia supplied the Chelating Sepharose Fast Flow resin and the reagents for fluorescence dideoxy sequencing that accompany their Automated Laser Fluorescent (A.L.F.) DNA sequencer. The oligonucleotides for the polymerase chain reaction (PCR) were purchased from Genset, while the oligonucleotides for site-directed mutagenesis and sequencing were synthesized in-house on an Applied Biosystems 392 RNA/DNA synthesizer. Fluorescent primers were prepared with FluorePrime, a fluorescein amidite, also from Pharmacia.

Bacterial strains - *Escherichia coli* strain DH5αF' was used in the cloning procedures, *E. coli* strain "dut^- ung^-" for mutagenesis, and *E. coli* strain BL21.DE3.pLysS was used for protein overexpression.

Construction of pET-23a/BT-trans- Plasmid DNA used for cloning and sequencing was prepared through either the alkaline lysis method (17) or with a kit supplied by QIAGEN. DNA encoding the BTA heavy chain was isolated from genomic DNA (18). This construct was prepared as a linear strand template for PCR. Oligonucleotides were designed against the translocation domain to include two unique restriction sites as well as encode for a C-terminal Myc epitope tag and polyhistidine tail. PCR products were gel-purified and extracted using the QIAGEN gel extraction kit. Following resuspension in TE (10 mM Tris, 1 mM EDTA, pH 8.0), the DNA was ligated into a pGEMT vector (Promega) by A/T overlaps and sequenced to check for correct PCR amplification. The DNA was then digested with Nde 1 and Xho 1 and ligated into the pET-23a vector (Novagen).

Site-Directed Mutagenesis- The pET-23a/BT-trans plasmid was transformed into a dut$^-$ ung$^-$ strain of *E. coli.* Site-directed mutagenesis was performed using standard protocols for manipulating single-stranded uracil-containing DNA (17).

Expression and Purification of the Translocation Domain- Expression of the BT-trans domain was under the control of the T7 polymerase promoter in pET-23a. Initially, expression was done in 1 L shaker flasks containing LB/carb/CAP (Luria-Bertani medium (17) containing 50 μg/mL carbenicillin and 34 μg/mL chloramphenicol). The media was inoculated with a single colony of BL21.DE3.pLysS carrying the desired plasmid, incubated with shaking at 37 °C and, at an O.D.=0.6, induced with 1 mM IPTG. In later experiments, the cells were grown in a 200 L fermentor with all reagents scaled up proportionally. Starting with 60 grams of cell paste, the bacterial pellet was resuspended in 30 mL of binding buffer (500 mM NaCl, 5 mM imidazole, 0.3 mM methionine, and 20 mM Tris, pH 7.9) Protease inhibitors were added to final concentrations of 0.12 mg/mL phenylmethylsulfonyl fluoride (PMSF), 6.7 μg/mL pepstatin A, and 6.7 μg/mL leupeptin. Additionally, 200 μL of 1 M $MgCl_2$ and small amounts of DNAse were added. Cells were lysed using a French press and the soluble and insoluble portions were separated by centrifugation. The pellet was washed with 30 mL binding buffer in the presence of 1 mL 0.5 M EDTA and recentrifuged prior to resuspension in a total volume of 30 mL binding buffer in 1% n-lauroyl sarcosine. Following centrifugation, the supernatant was filtered and further purified using metal affinity chromatography. A column packed with metal chelating resin was charged with 50 mM of either $NiSO_4$ or $CuSO_4$. The column was pre-equilibrated with the binding buffer plus 1 % Sarcosyl solution before loading the protein. Following an extended wash step, the protein was eluted off the column by increasing the imidazole concentration to 500 mM.

Circular Dichroism (CD) - All CD spectra were obtained on a Aviv 62DS spectropolarimeter with a Peltier temperature-controlled sample holder and with a 1-cm path length cuvette. Potassium phosphate buffers were prepared at pH 3, 6, 7, and 8. Potassium acetate was used as the buffer at pH 4 and 5.

Enzyme linked immunosorbent assay (ELISA) - Microtiter plates (Falcon 3912) were incubated with 50 μL of the translocation domain at 10 μg/mL in PBS (25 mM NaH_2PO_4, 125 mM NaCl, pH 7.0) at 4 °C overnight. After

washing once with PBS, wells were incubated with 50 µL bacterial supernatant containing native E-tagged single chain variable fragment (scFv). Antibodies were detected using an anti-E tag antibody (1 mg/mL) (Pharmacia), followed by peroxidase-conjugated anti-mouse Fc antibody (Sigma), and 2,2'-azinobis(3-ethylbenzthiazoline-sulfonic acid) as substrate as described (19).

Crystal Growth - Initial crystals were found from an incomplete factorial grid (20) using Crystal Screens I and II (Hampton Research). Crystals were grown at 4 °C and 25 °C by the hanging drop vapor diffusion method from a starting protein concentration of 7.8 mg/mL.

Sequence homology - Sequence homology between the clostridial toxins was determined by the BLAST algorithm (21) to align sequences in the SwissProt database.

RESULTS AND DISCUSSION

Construction of a BT-trans Overexpression System and Related Mutations - Primers were designed to isolate the translocation domain as residues 449-870 (Fig. 1a) as determined in the complete amino acid sequence of the holotoxin (22). This construct's sequence differs from the target sequence by an N-terminal methionine to start translation, a C-terminal Myc epitope tag to facilitate detection by Western blot analysis, and a C-terminal polyhistidine tag to enable purification by metal affinity chromatography (Fig. 1b). The initial construct contains two cysteines which do not form a disulfide bond in the native protein since the N-terminal cysteine is known to form the disulfide bridge with the catalytic domain. While the initial cysteine-containing construct was shown to overexpress, unwanted inter- or intra-molecular disulfides were prevented by replacing the two cysteines with alanines. This construct, BT-trans (C454A, C791A), was prepared by site-directed mutagenesis, verified by sequencing, and shown to express in similar yields to the original construct. The protein identity was verified by Western blot analysis (Fig. 2, Lane 1). Here, the upper 50-kDa band corresponds to the translocation domain. The lower band at 40-kDa was a result of proteolytic cleavage and was removed through the incorporation of protease inhibitors in the purification. Interestingly, the lower band at 30-kDa was a result of an internal methionine codon located six bases downstream from a Shine-Dalgarno sequence in which only one of eight bases differed from the canonical sequence (Fig. 1c). This co-translational contaminant was eliminated by introducing silent mutations in the internal Shine-Dalgarno sequence by site-directed mutagenesis. These changes were again, verified by sequencing, and new Western blot analysis showed the complete elimination of this contaminant (Fig 2. Lane 2).

Purification of the BT-translocation Domain - The protein was expressed to the insoluble portion of the cell. After experimenting with a number of salts, denaturants and detergents, 1% n-lauroyl sarcosine, a zwitterionic detergent, was found to be the most effective means of solubilizing the protein. The resolubilized protein was then further purified by metal affinity chromatography. The sample (Fig. 3, Lanes 3-6) is believed to be greater than

95% pure as assessed by Coomassie and silver stain gel electrophoresis. This expression and purification protocol yields 1 mg pure protein for every 1 g of cell paste. The translocation domain is folded and stable in solution as shown by CD, ELISA and crystallization experiments.

CD spectropolarimetry - Since the recombinant protein was isolated from the insoluble fraction, it is especially important to determine if the protein is folded. Far-UV CD spectropolarimetry of the recombinant protein showed a spectrum indicative of secondary structure as evidenced by the minima at 208 and 222 nm (Fig. 4). Similar wavelength scans were taken in 1 unit pH increments from 3 to 8. Two different buffering agents were required to achieve the optimal pKa's. It was interesting to observe that the spectra at pH 3, 6, 7 and 8 were identical. Unfortunately, spectra could not be attained at pH 4 and 5, as the protein was insoluble under these conditions. This 4-5 pH range is also the pH range of the endosome when the putative conformational change occurs. The calculated pI of the protein domain is 3.6. While it is not surprising that the protein would become more insoluble as it rearranges itself to interact with the membrane, further efforts will be made to find conditions where these changes can be monitored by biophysical techniques.

ELISA- Further evidence in support of a properly folded structure comes from work in mapping antibodies binding the holotoxin to the individual domains[2] . Of the forty scFv's that mapped to the holotoxin, three mapped exclusively to the translocation domain. ELISA's on these three antibodies were performed on protein purified as described above and on the same protein after heat denaturation. The denatured protein showed no signal by ELISA, indicating that the antibodies recognize a conformational epitope as opposed to a linear one.

Preliminary crystallization results - The final piece of evidence in favor of structured protein was that the protein has been shown to crystallize in the presence of 100 mM magnesium formate, 100 mM Tris pH 8.5, and 1 mM sodium azide (Fig. 5). While not yet of diffraction quality, the ability to grow crystals indicates a specific molecular packing arrangement unlikely for denatured proteins. Crystals were confirmed to be protein by staining with methylene blue and by analysis of crystals by SDS-PAGE.

---

[2] Chen, F., Kuziemko, G., Amersdorfer, P., Wong, C., Marks, J. D., and Stevens, R. C. (1996) *Infect. Immun.* (submitted)

Conclusion - The BT translocation domain is part of a soluble holo-protein that does not become activated until it enters the endosome. Once inside the endosome, the low pH induces unknown conformational changes in the translocation domain that allow it to merge with the endosomal cell membrane and carry the 50-kDa catalytic domain to the cytosol. Once in the cytosol, the protease is able to perform the final function of the toxin, the inhibition of synaptic vesicle fusion resulting in nerve paralysis. Efforts to understand the basic mechanism of toxin translocation events have been undertaken in a number of systems, including DT (12-16), *Pseudomonas* exotoxin A (PE) (23), Ricin (24), and Shiga toxin (25). However, none of these other toxins can carry such a large 50-kDa protein to the cytosol. The ability to produce the translocation domain in suitable amounts provides the opportunity to study the translocation event in BT. Since botulinum neurotoxin is able to carry such a large protein to the cytosol, the translocation domain could possibly be harnessed to deliver other large proteins to their targets within the cytosol, analogous to immunotoxin and protein design strategies pursued previously with DT and PE (26-28). A further understanding of the translocation mechanism will greatly aid in this endeavor.

Acknowledgments - We thank Carl Chen for the initial genomic DNA cloning and Flora Chen for performing the ELISA experiments.

REFERENCES:

1. DasGupta, B.R. and Sugiyama, H. (1972) *Biochem. Biophys. Res. Commun.* **48,** 108-112
2. Sugiyama, H. (1980) *Microbiol. Rev.* **44,** 419-448
3. Simpson, L.L. (1980) *J.Pharmacol. Exp. Ther.* **212,** 16-21
4. Dolly, J.O., Black, J., Williams, R.S. and Melling, J. (1984) *Nature* **307,** 457-460
5. Blewitt, M. G., Chung, L. A., and London, E. (1985) *Biochemistry* **24,** 5458-5464
6. Dumont, M. E., and Richards, F. M. (1988) *J. Biol. Chem.* **263,** 2087-2097
7. Hoch, D. M., Romera-Mira, M., Ehrlich, B. E., Finkelstein, A., DasGupta, B. R., and Simpson, L. L. (1985) *Proc. Natl. Acad. Sci U. S. A.* **82,** 1692-1696
8. Schmid, M. F., Robinson, J. P., and DasGupta, B. R. (1993) *Nature* **364,** 827-830
9. Blasi, J., Chapman, E.R., Link, E., Binz, T., Yamasaki, S., De Camilli, P., Sudhof, T.C., Niemann, H. and Janh, R. (1993) *Nature* **365,** 160-163
10. Burgen, A.S.V., Dickens, F. and Zalman, L.J. (1949) *J.Physiol. (London)* **109,** 10-24
11. Choe, S., Bennett, M. J., Fujii, G., Curmi, P. M. G., Kantardjieff, K. A., Collier, R. J., and Eisenberg, D. (1992) *Nature* **357,** 216-222
12. Johnson, V. G., Nicholls, P. J., Habig, W. H., and Youle, R. J., (1993) *J. Biol. Chem.* **268,** 3514-3519
13. Madshus, I. H. (1994) *J. Biol. Chem.* **269,** 17723-17729
14. vanderSpek, J., Cassidy, D., Genbauffe, F., Huynh, P. D., and Murphy, J. R. (1994) *J. Biol. Chem.* **269,** 21455-21459
15. Silverman, J. A., Mindell, J. A., Finkelstein, A., Shen, W. H., and Collier, R. J. (1994) *J. Biol. Chem.* **269,** 22524-22532
16. Zhan, H., Oh, K. J., Shin, Y.-K., Hubbell, W. L., and Collier, R. J. (1995) *Biochemistry* **34,** 4856-4863
17. Maniatis, T., Fritsch, E. F., and Sambrook, J. (1982) *Molecular Cloning: A Laboratory Manual,* Cold Spring Harbor Laboratory, Cold Spring Harbor, NY
18. Betley, M. J., Somers, E., and DasGupta, B.R. (1989) *Biochem. Biophys. Res. Commun.* **162,** 1388-1395
19. Schier, R., Bye, J., Apell, G., McCall, A., Adams, G. P., Malmquist, M., Weiner, L. M., and Marks, J. D. (1996) *J. Mol. Bio.* **255,** 28-43
20. Jancarick, J., and Kim, S. H. (1991) *J. Appl .Crystallogr.* **24,** 409-411
21. Altschul, S. F., Gish, W., Miller, W., Myers, E. W., and Lipman, D. J. (1990) *J. Mol. Bio.* **215,** 403-410
22. Binz, T., Kurazono, H., Wille, M., Frevert, J., Werners, K. & Niemann, H. (1990) *J. Biol. Chem.* **265,** 9153-9158
23. Theuer, C. P., Buchner, J., FitzGerald, D., and Pastan, I. (1993) *Proc. Natl. Acad. Sci U. S. A.* **90,** 7774-7778
24. Beaumelle, B., Alami, M., and Hopkins, C. R. (1993) *J. Biol. Chem.* **268,** 23661-23669
25. Sandvig, K., Garred, O., Prydz, K., Kozlov, J. V., Hansen, S. H., van Deurs, B. (1992) *Nature* **358,** 510-512
26. Stenmark, H., Moskaug, J. O., Madshus, I. H., Sandvig, K., and Olsnes, S. (1991) *J. Cell . Biol.* **113,** 1025-1032
27. Madshus, I. H., Olsnes, S., and Stenmark, H. (1992) *Infect. Immun.* **60,** 3296-3302
28. Prior, T. I., FitzGerald, D. J., and Pastan, I. (1992) *Biochemistry* **31,** 3555-3559

FIGURE LEGENDS:

FIG. 1. BT-Translocation Domain Constructs in pET23a. **a)** The three functional domains of BT. **b)** The original PCR product was cloned into pET-23a using Nde 1 and Xho 1. **c)** Site-directed mutagenesis was used to convert cysteines to alanines and to introduce silent mutations in the internal Shine-Dalgarno sequence.

FIG. 2. Western blotting to confirm protein identity. SDS-PAGE was followed by transfer to nitrocellulose, sequential incubation with anti-Myc and anti-mouse Horseradish peroxidase antibodies, and detection by ECL.

FIG. 3. SDS-PAGE to assess expression and purity of BT-trans. Electrophoresis was performed on a 10% acrylamide gel under reducing conditions. Protein bands were visualized by silver staining. Lanes 1 through 6 show the purification of the BT-trans (with all mutations incorporated) by metal affinity chromatography. Lane 1 shows what was loaded on the column, lane 2 represents the flow-through, and lanes 3-6 show the purified protein after elution with 500 mM imidazole.

FIG. 4. Far-UV CD spectrum of BT-translocation domain. Wavelength scan was taken at 25 °C using a 1-cm path length strain-free cuvette (BT-trans at 30 μg/mL, 5 mM potassium phosphate, pH 7.0, 5 mM KCl)

FIG. 5. Preliminary crystallization of BT-translocation domain. The protein was concentrated to 7.8 mg/mL and crystallized in the presence of 100 mM magnesium formate. Crystals were grown at 4 °C in 2 days by the hanging drop method.

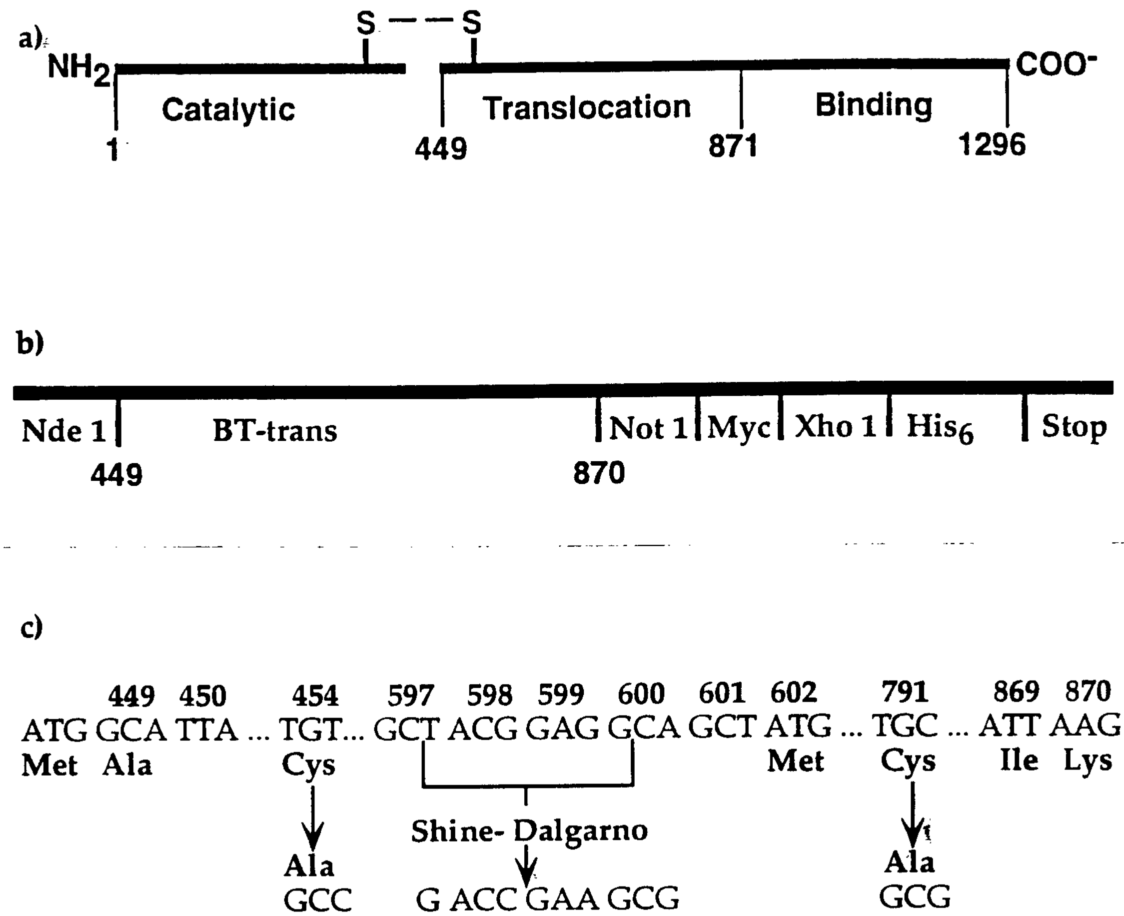
a)
S — — S
NH2
COO-
Catalytic
Translocation
Binding
1
449
871
1296
b)
Nde 1
BT-trans
Not 1
Myc
Xho 1
His6
Stop
449
870
c)
449 450 454 597 598 599 600 601 602 791 869 870
ATG GCA TTA ... TGT... GCT ACG GAG GCA GCT ATG ... TGC ... ATT AAG
Met Ala Cys Met Cys Ile Lys
Shine- Dalgarno
Ala
GCC
G ACC GAA GCG
Ala
GCG

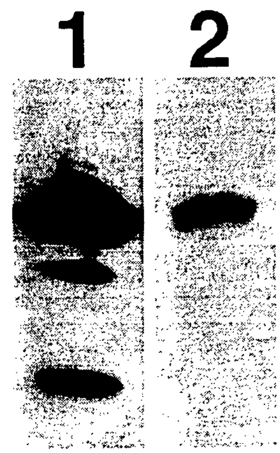
1
2

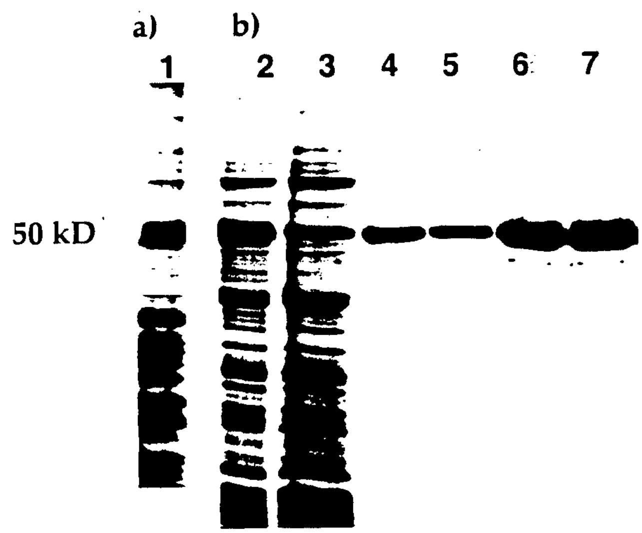
a)
b)
1
2
3
4
5
6
7
50 kD

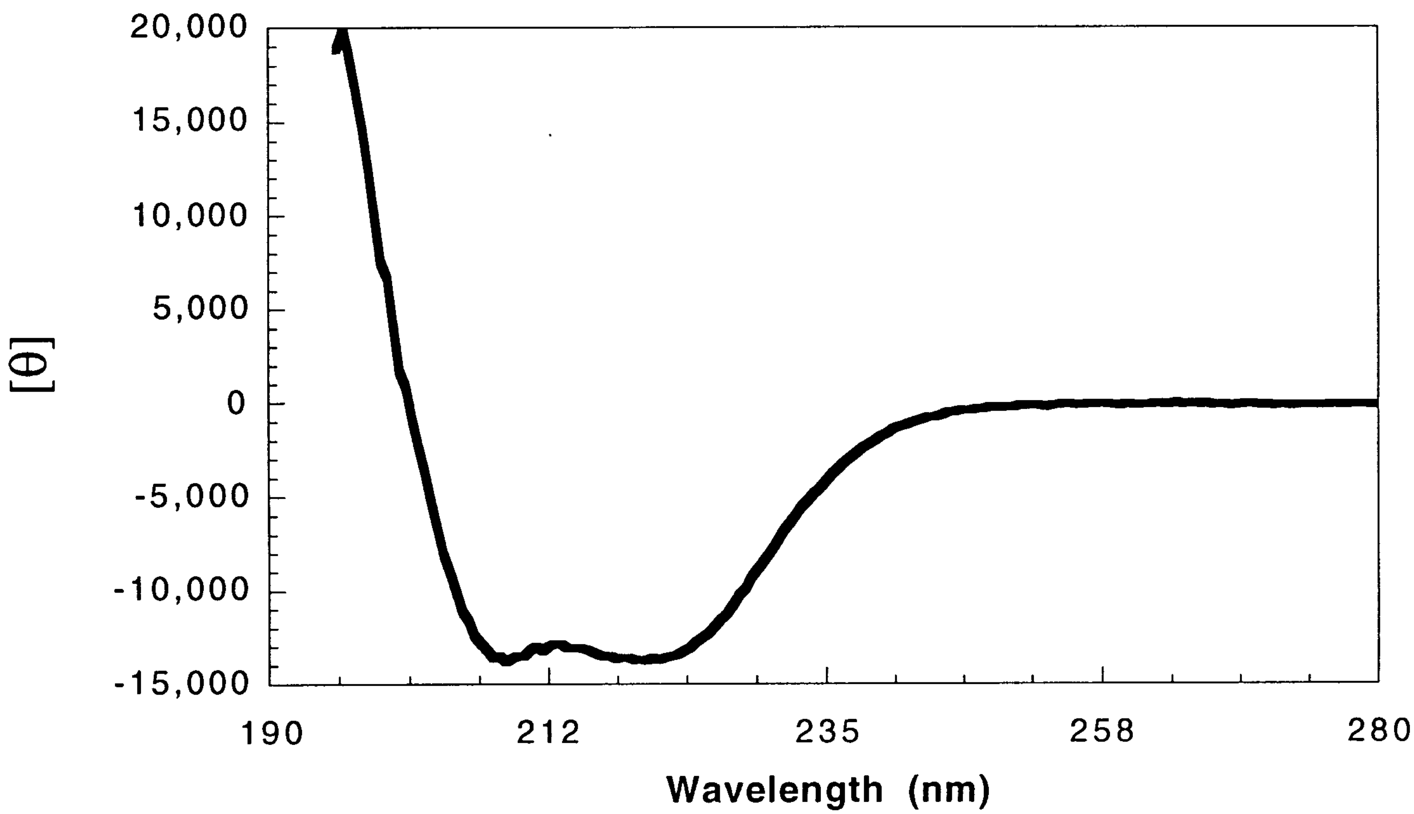
[θ]
20,000
15,000
10,000
5,000
0
-5,000
-10,000
-15,000
190
212
235
258
280
Wavelength (nm)

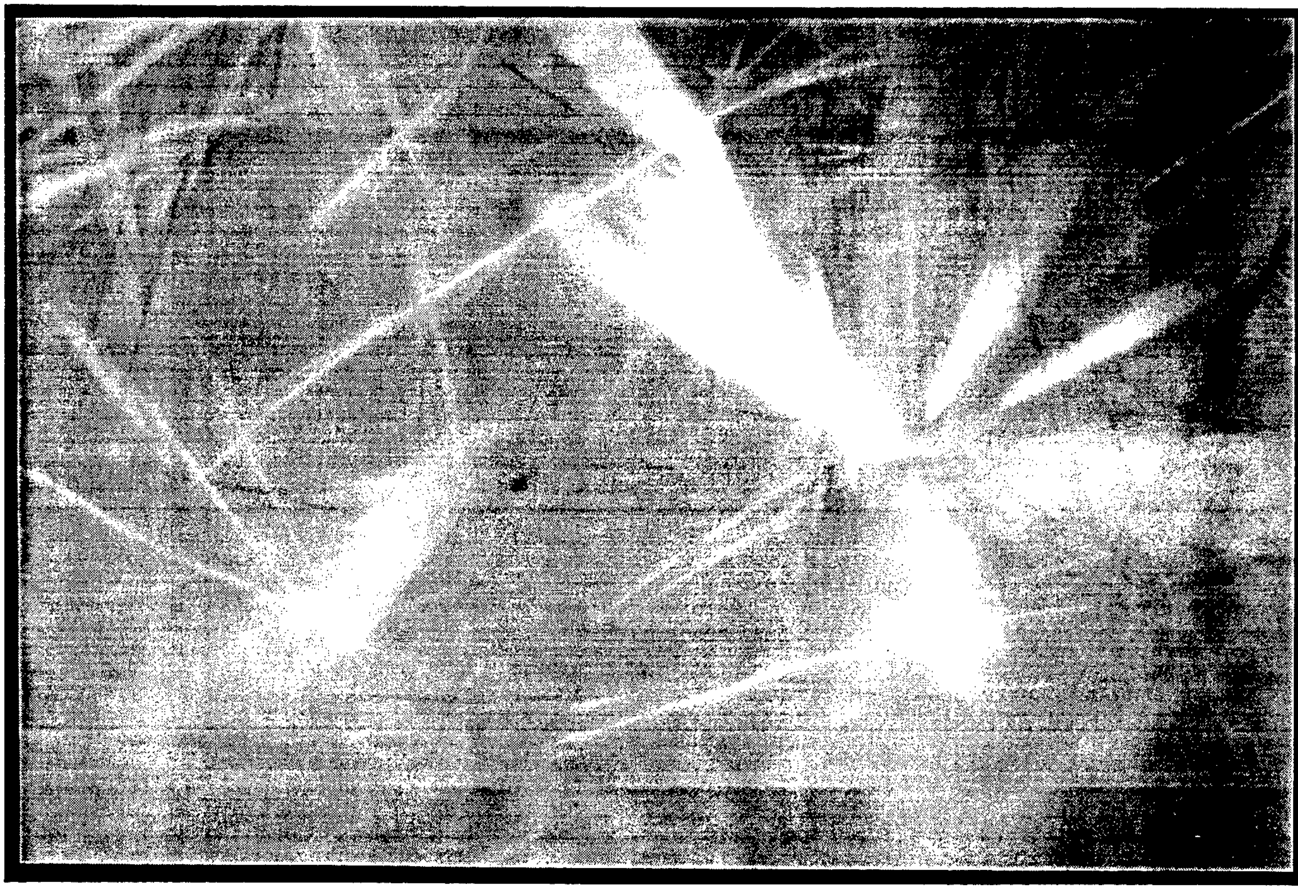

INFECTION AND IMMUNITY, May 1997, p. 1626–1630 Vol. 65, No. 5
0019-9567/97/$04.00+0

Antibody Mapping to Domains of Botulinum Neurotoxin Serotype A in the Complexed and Uncomplexed Forms

FLORA CHEN,[1] GEOFFREY M. KUZIEMKO,[2] PETER AMERSDORFER,[3] CINDY WONG,[3] JAMES D. MARKS,[3]* AND RAYMOND C. STEVENS[1,2]*

Graduate Group in Biophysics[1] and Department of Chemistry,[2] University of California, Berkeley, California 94720, and Departments of Anesthesia and Pharmaceutical Chemistry, University of California, San Francisco, San Francisco, California 94110[3]

Received 8 November 1996/Returned for modification 13 January 1997/Accepted 7 February 1997

The domain organization of the botulinum neurotoxin serotype A was studied by using antibody mapping of 44 monoclonal single-chain variable fragments. The analysis was carried out on (i) the individual domains of botulinum neurotoxin holotoxin (binding, translocation, and catalytic), (ii) botulinum neurotoxin holotoxin, (iii) the botulinum neurotoxin holotoxin in complex with the nontoxic portion, and (iv) botulinum neurotoxin holotoxin and nontoxic portion of the complex recombined in vitro. All 44 antibodies mapped to individual domains of botulinum neurotoxin. Forty of the 44 single-chain variable fragments bound the botulinum neurotoxin holotoxin relative to the isolated domains, suggesting that 4 epitopes are covered when the individual domains are in the holotoxin form. Only 20 of the antibodies showed a positive reaction to the toxin while in complex with the nontoxic portion. All of the covered epitopes were mapped to the binding domain of botulinum neurotoxin, which suggested that the binding domain is in direct contact with the nontoxic portion in the complex. Based on the antibody mapping to the different domains of the botulinum neurotoxin holotoxin and the entire complex, a model of the botulinum neurotoxin complex is proposed.

The anaerobic bacterium *Clostridium botulinum* produces seven serotypes of neurotoxin, classified A through G (26). The neurotoxin, serotype A, can be purified as a 900-kDa complex consisting of a 150-kDa toxic component (botulinum neurotoxin [BT]), and a 750-kDa nontoxic component (hemagglutinin [HA]) (3). The BT inhibits cholinergic vesicle docking at the neuromuscular junction, resulting in flaccid paralysis (23), and most commonly intoxicates by oral ingestion. The three 50-kDa functional domains of BT—binding (13), translocation (2), and catalytic (1a)—allow the toxin to bind to a cell surface receptor, pass across the membrane (23), and cleave a protein involved in vesicle docking, respectively (9). Sugii and coworkers (24) have shown that the HA-BT complex has a higher oral toxicity in rats than the BT alone. The 750-kDa HA has been shown to have an agglutination ability (15) and is thought to protect the toxin from the extreme pH and proteases in the gut (25).

Little structural information is known about BT, HA-BT, or the interaction between BT and HA. The literature contains examples of antibodies used to detect various serotypes of BT (7, 12, 14, 27), but no mapping of the BT domains in the HA-BT complex has been carried out. Sugiyama and coworkers (27) showed that polyclonal antibodies to type A HA-BT complex recognized epitopes predominantly from the HA and not the BT. Monoclonal antibodies developed by Kozaki and coworkers recognized the light chain of the BT that causes infant botulism and the light chain of BT serotype A (14). However, the antibodies to the infant botulism BT heavy chain did not recognize the BT serotype A heavy chain. Studies using polyclonal antibodies to the toxin detected BT at very low concentrations but did not provide specific information about the relationship between the BT and HA (7, 12). We probed the structure of the HA-BT complex by using a panel of 44 unique monoclonal single-chain variable fragments (scFv) derived from combinatorial phage antibody libraries (1, 28).

We used enzyme-linked immunosorbent assays (ELISAs) to identify 44 scFv that bind to different domains of botulinum neurotoxin serotype A. ELISAs were performed on purified BT, the purified BT domains, HA, HA-BT complex, and recombined HA-BT in vitro. Based on our results, we propose a model to illustrate the interaction between BT and HA. The model could act as a guide for the design of neutralizing antibodies and may explain how the HA protects the BT from proteolytic and pH attack.

MATERIALS AND METHODS

Purification of HA-BT complex, BT, and BT domains. The HA-BT complex (Hal strain) was obtained as an ammonium sulfate precipitate from purified bacterial supernatant at a concentration of 3.3 mg/ml in 50 mM sodium citrate (pH 5.5) (5). Before use, the HA-BT complex was centrifuged at 26,890 × *g* (Dupont Sorvall RC-5B centrifuge) for 15 min and dialyzed against saline (0.68 M sodium citrate, 0.145 M NaCl [pH 7.4]) with three buffer exchanges within an hour. Concentration was determined by A_{278} measurements (1.66 arbitrary units/mg ml^{-1}), using a Shimadzu UV-160 spectrophotometer (11).

The HA was purified in two steps by using a modification of a published procedure (4). Forty-five milligrams of ammonium sulfate precipitate of HA (0.42 g/ml) was centrifuged at 26,890 × *g*. The pellet was dissolved in 20 ml of 70 mM Tris-HCl (pH 7.2) and dialyzed overnight. The dialyzed solution was centrifuged at 26,890 × *g* for 15 min and applied onto a DEAE-Sepharose column (1.5 by 24 cm; Pharmacia, Uppsala, Sweden) that was equilibrated with 70 mM Tris-HCl (pH 7.2). The column was washed with 100 ml of 70 mM Tris-HCl (pH 7.2) and the HA was eluted with 70 mM Tris-HCl–0.2 M NaCl (pH 7.2). The fractions containing HA were combined and run on an SP-Sepharose column (1.5 by 21 cm) (Pharmacia, Uppsala, Sweden) equilibrated with 70 mM Tris-HCl (pH 7.2). Since residual BT adheres to the column matrix at this pH, the HA was collected in the flowthrough. The concentration of protein was determined by A_{278} measurements (11).

The BT was purified as described previously (5) and stored as a 10-mg/ml solution in 10 mM HEPES (pH 7.0)–0.1 M KCl–2 mM sodium azide. The binding domain of BT type A, expressed in *Escherichia coli* and purified by immobilized metal affinity chromatography using a C-terminal His$_6$ tag, was

* Corresponding author. Mailing address for James D. Marks: Departments of Anesthesia and Pharmaceutical Chemistry, University of California, San Francisco, SFGH Room 3C-38, 1001 Potrero, San Francisco, CA 94110. Phone: (415) 206-3256. Fax: (415) 206-3253. E-mail: jim_marks@quickmail.ucsf.edu. Phone for R. C. Stevens: (510) 643-8285. Fax: (510) 643-9290. E-mail: Stevens@adrenaline.berkeley.edu.

Appendix B

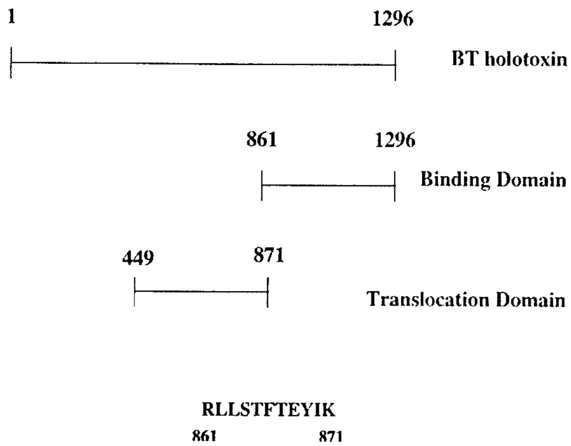

FIG. 1. Diagram illustrating the sequence overlap between the translocation and binding domain constructs. The top line represents the sequence of BT from the N terminus (residue 1) to the C terminus (residue 1296). The bottom two lines depict the C-terminal 11 residues from the translocation domain construct overlapping the N-terminal 11 residues of the binding domain (18, 19).

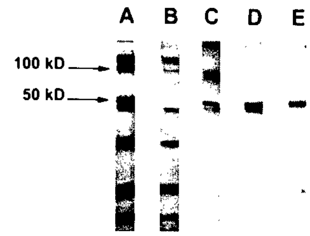

FIG. 2. SDS-PAGE analyses of column chromatography. Lanes: A, HA-BT complex; B, purified HA; C, purified BT; D, purified binding domain; E, purified translocation domain.

purchased from Ophidian Pharmaceuticals, Inc. (Madison, Wis.). The translocation domain (residues 449 to 872) of BT type A was expressed in *E. coli* and purified by immobilized metal affinity chromatography using a C-terminal His_6 tag (14a). The 11 C-terminal residues of the translocation domain overlap the 11 N-terminal residues of binding domain (18, 19) (Fig. 1). The polypeptide composition of each of the different batches of purified protein was analyzed on 12% polyacrylamide gels as described by Fling and Gregerson (8).

Antibodies. ScFv antibody fragments were selected from four different combinatorial phage antibody libraries (1, 28). Briefly, scFv phage antibody libraries were constructed from the immunoglobulin heavy (V_H)- and light (V_L)-chain variable regions of mice immunized with purified holotoxin (library 1); mice immunized with binding domain (library 2); humans immunized with pentavalent botulinum toxoid (Centers for Disease Control and Prevention) (library 3); nonimmunized human volunteers (library 4). Libraries 1 and 3 were constructed in the vector pCANTAB5E (Pharmacia), and library 2 was constructed in pHEN-1 (10). Specific scFv were isolated by selecting the libraries on either holotoxin or binding domain immobilized on polystyrene or in solution. The specificity of the isolated antibodies for the holotoxin or the binding domain was confirmed by ELISA on the relevant antigen and a panel of irrelevant antigens (1, 28). The number of unique scFv was determined by *Bst*N1 fingerprinting, followed by DNA sequencing of the V_H and V_L genes. Additional unique scFv were isolated from a 9.7×10^9-member nonimmune library in pHEN-1 (10) constructed from human V_H and V_L genes.

For structural mapping of the HA-BT complex, BT, and BT domains by ELISA, native scFv was expressed from the appropriate phagemid in *E. coli* HB2151 (10). The amber codon between the scFv gene and gene 3 permits expression of native scFv in a nonsuppressor *E. coli* strain (HB2151). scFv binding was detected by using the epitope tag at the C terminus of the scFv (E tag for scFv in pCANTAB5E and Myc tag for scFv in pHEN-1). Since both the scFv in pHEN-1 and the translocation domain have a C-terminal Myc tag, ELISA on the translocation domain was performed with scFv fused to phage, and detection was achieved by using HRP/anti-M13 conjugate (Pharmacia).

Expression of native scFv (6) in the phagemid vectors (pHEN-1 and pCANTAB5E) was performed in 96-well microtiter plates as described previously (16), with the following exception: after overnight growth and expression at 25°C, 50 μl of 0.5% Tween 20 was added to each well and the plates were incubated for 4 h at 37°C with shaking to induce bacterial lysis and increase the concentration of scFv in the bacterial supernatant. Supernatants containing native scFv were used for ELISA. To prepare phage for ELISA, single ampicillin-resistant colonies were transferred into microtiter plate wells containing 100 μl of 2×YT medium (16 g of Bacto Tryptone, 10 g of Bacto Yeast Extract, 5 g of NaCl, 1 liter of deionized H_2O) supplemented with 1 mM ampicillin (Sigma, St. Louis, Mo.) and 0.1% glucose. After 3 h of growth at 37°C to an A_{600} of approximately 0.5 arbitrary unit, VCSM13 helper phage (2.5×10^8 phage particles) was added, and the cells were incubated for 1 h at 37°C. Subsequently, kanamycin was added to a final concentration of 25 μg/ml, and the bacteria were grown overnight at 37°C. Supernatants containing phage were used for ELISA.

ELISA. Microtiter plates (Falcon 3912) were incubated with 50 μl of antigen (10 μg/ml except for the binding domain, in which case 5 μg/ml was used) in phosphate-buffered saline (PBS; 25 mM NaH_2PO_4, 125 mM NaCl [pH 7.0]) at 4°C overnight. After being washed once with PBS, wells were incubated with 50 μl of bacterial supernatant containing either native scFv or scFv fused to phage. Myc-tagged scFv were detected with mouse monoclonal antibody 9E10 (1 μg/ml; Santa Cruz Biotechnology) (17), and E-tagged scFv were detected by using anti-E tag antibody (1 mg/ml; Pharmacia), followed by peroxidase-conjugated anti-mouse Fc antibody (Sigma), with 2,2′-azinobis(3-ethylbenzthiazoline-sulfonic acid) as the substrate as described previously (21). Binding of scFv phage to antigens was detected with peroxidase-conjugated anti-M13 antibody (Pharmacia) as described elsewhere (20).

Recombination. The purified BT and HA were incubated at a 1:1 molar ratio for at least 24 h in 70 mM Tris-HCl (pH 7.2) at a protein concentration of 0.1 mg/ml. The mixture was stored at 4°C until diluted in PBS for coating ELISA plates.

RESULTS

Purification of antigens. After column chromatography, the purities of HA-BT complex, BT, and HA were ascertained by sodium dodecyl sulfate-polyacrylamide gel electrophoresis (SDS-PAGE) to be relatively free of contaminants (Fig. 2). The BT appeared as two bands, separated due to the reducing environment of the gel loading buffer—a 50-kDa light chain consisting of catalytic domain and a 100-kDa heavy chain consisting of translocation and binding domains. The HA-BT complex runs as nine bands that make up the BT and large HA. Purified HA appears identical to the HA-BT complex minus the 50-kDa polypeptide from the light chain of BT. A small amount of 100-kDa band from the heavy chain of BT was present in the HA. This residual BT was not enough to produce a positive signal for HA on ELISA. Binding and translocation domains, expressed in *E. coli* were also tested for purity by SDS-PAGE.

Antibody isolation and initial characterization. scFv were isolated by selection of phage libraries on immobilized purified BT or purified recombinant binding domain. The antibodies recognize only native protein and not denatured protein. Thus, the antibodies bound according to structure and not sequence libraries (1, 28). After three rounds of selection, initial scFv characterization by ELISA on BT and DNA sequencing of the V_H and V_L genes yielded 44 unique scFv (Table 1).

Structural mapping of BT, HA-BT complex, and BT domains. The forty-four scFv recognized the individual domains of BT, and none bound to HA alone (Table 1). Of the 44 scFv, 24 mapped to the binding domain and 3 mapped to the translocation domain (Table 1). In addition, two antibodies mapped to both the binding and translocation domains. These two scFv presumably bound to the 11-amino-acid overlap at the C terminus of the translocation domain and the N terminus of the binding domain (Fig. 1). Alternatively, cross-reactivity could result from binding to a four-amino-acid sequence (-KYVD-) that is homologous for residues 855 to 858 of the translocation domain and 1121 to 1124 of the binding domain. Thus, 26 scFv recognized the binding domain and 5 bound the translocation domain construct. The remaining 15 scFv presumably bound to the catalytic domain, though this was not tested directly due to lack of purified catalytic domain. Some of these 15 may recognize epitopes that are shared between domains.

TABLE 1. ELISA absorbances of scFv to type A neurotoxin[a]

Antibody	OD_{405} (avg ± SD)				
	BT	HA-BT	Binding domain	Translocation domain	RR
3d12	2.303 ± 0.682	0.659 ± 0.072	2.260 ± 0.489		1.181 ± 0.303
3a6	2.053 ± 0.768	0.660 ± 0.083	1.775 ± 0.263		1.160 ± 0.322
3d4	0.964 ± 0.192	0.913 ± 0.192			1.091 ± 0.108
4a4	0.950 ± 0.135	0.905 ± 0.045			1.195 ± 0.071
3a2	1.091 ± 0.192	0.936 ± 0.138			1.204 ± 0.234
3e3	1.106 ± 0.170	0.987 ± 0.158			1.229 ± 0.255
3e8	1.058 ± 0.358	0.941 ± 0.097			1.145 ± 0.245
3a11	1.036 ± 0.298	0.934 ± 0.108			1.248 ± 0.157
3e7	1.022 ± 0.262	0.945 ± 0.156			1.218 ± 0.153
3h3	1.143 ± 0.396	0.838 ± 0.380			1.037 ± 0.316
3a1	1.019 ± 0.300	0.943 ± 0.148			1.206 ± 0.167
w3	2.083 ± 0.523	1.544 ± 0.192			1.925 ± 0.267
w42	1.796 ± 0.409	1.400 ± 0.223			1.721 ± 0.270
g23	1.875 ± 0.403	1.460 ± 0.194			1.795 ± 0.183
g3	1.287 ± 0.329	0.890 ± 0.298			1.290 ± 0.174
g11	1.200 ± 0.326	0.956 ± 0.192			1.285 ± 0.100
w7	1.552 ± 0.269	1.199 ± 0.273		1.182 ± 0.121	1.606 ± 0.393
w9	1.492 ± 0.376	1.239 ± 0.247		1.201 ± 0.152	1.510 ± 0.194
g7	1.072 ± 0.481	1.106 ± 0.327		0.590 ± 0.105	1.422 ± 0.261
w20	1.557 ± 0.530		1.713 ± 0.349		1.089 ± 0.053
w36	1.302 ± 0.418		1.362 ± 0.300		0.680 ± 0.026
w43	1.421 ± 0.253	1.002 ± 0.109			1.283 ± 0.334
g53	1.193 ± 0.321		1.700 ± 0.242		0.685 ± 0.095
g57	1.647 ± 0.409		1.423 ± 0.521		0.761 ± 0.117
c9	1.560 ± 0.460		1.690 ± 0.229		0.889 ± 0.213
c15	1.936 ± 0.535		1.988 ± 0.458		1.079 ± 0.358
s25	1.395 ± 0.363		1.369 ± 0.435		
3f6	1.332 ± 0.338		1.553 ± 0.272		0.811 ± 0.142
2a2	0.816 ± 0.297		1.172 ± 0.262		0.838 ± 0.033
2b10	0.858 ± 0.332		1.204 ± 0.408		0.661 ± 0.143
2b1	0.836 ± 0.121		1.247 ± 0.278	1.227 ± 0.505	0.566 ± 0.010
3e6	0.909 ± 0.109		1.190 ± 0.135		0.605 ± 0.165
2e6	0.838 ± 0.181		1.046 ± 0.171		
3d1	0.908 ± 0.192		1.009 ± 0.385		0.752 ± 0.072
2b6	0.652 ± 0.298		0.711 ± 0.213		
2h6	1.010 ± 0.326		1.261 ± 0.346		0.928 ± 0.004
2a8	0.994 ± 0.275		1.069 ± 0.398		0.908 ± 0.226
id5	0.738 ± 0.289		1.273 ± 0.228		0.716 ± 0.085
ie8	0.556 ± 0.339		0.921 ± 0.513	1.000 ± 0.405	0.654 ± 0.057
ig7	0.834 ± 0.174		1.113 ± 0.313		0.688 ± 0.077
3c3			0.621 ± 0.026		
2c3			0.740 ± 0.065		
3e2			0.427 ± 0.089		
3c5			0.743 ± 0.204		

[a] Values obtained with antigen coated at 10 μg/ml except for the binding domain, which was coated at 5 μg/ml. OD_{405}, optical density at 405 nm; RR, recombination of purified BT and HA. The antibodies were produced in the lab of James D. Marks. The values represent the averages of 13 plates coated with BT, 10 plates coated with HA-BT complex, 6 plates coated with binding domain, 6 plates coated with translocation domain, 5 plates coated with HA, and 4 plates coated with recombined BT and HA. The background was defined as the signal from plates containing antigen and primary and secondary antibodies. Values represent absorbances after background absorbance is subtracted. Blanks in columns represent absorbances below three times the background absorbance. These scFv were assumed not to bind the corresponding antigen. Since the ELISAs were performed using different batches of supernatant, the average absorbance of each plate was normalized to the average absorbance of the first plate for a particular antigen.

Forty scFv bound to the holotoxin (Table 1). Thus, four epitopes were covered when the individual domains came together to form the BT. Of these 40 scFv, 22 mapped to the binding domain and 3 mapped to the translocation domain. The remaining 15 scFv were deduced to recognize the catalytic domain (Table 1).

ELISA of scFv on the HA-BT complex permitted identification of BT epitopes which were inaccessible in the HA-BT complex. Twenty epitopes were covered when in the HA-BT complex. All of these covered epitopes were localized to the binding domain. Of the 22 scFv that mapped to the binding domain and BT, only 2 scFv bound to the HA-BT complex (Table 1). The three scFv that bound to translocation domain and BT also bound to the HA-BT complex (Table 1). The 15 scFv that mapped to catalytic domain in BT likewise bound to the HA-BT complex (Table 1).

DISCUSSION

Using antibodies to map the different domains of botulinum neurotoxin serotype A, we propose a model illustrating how the toxin may bind into the HA assembly. Forty-four scFv were produced to the BT and its domains. The antibodies specific to individual domains were used to map relative positions of

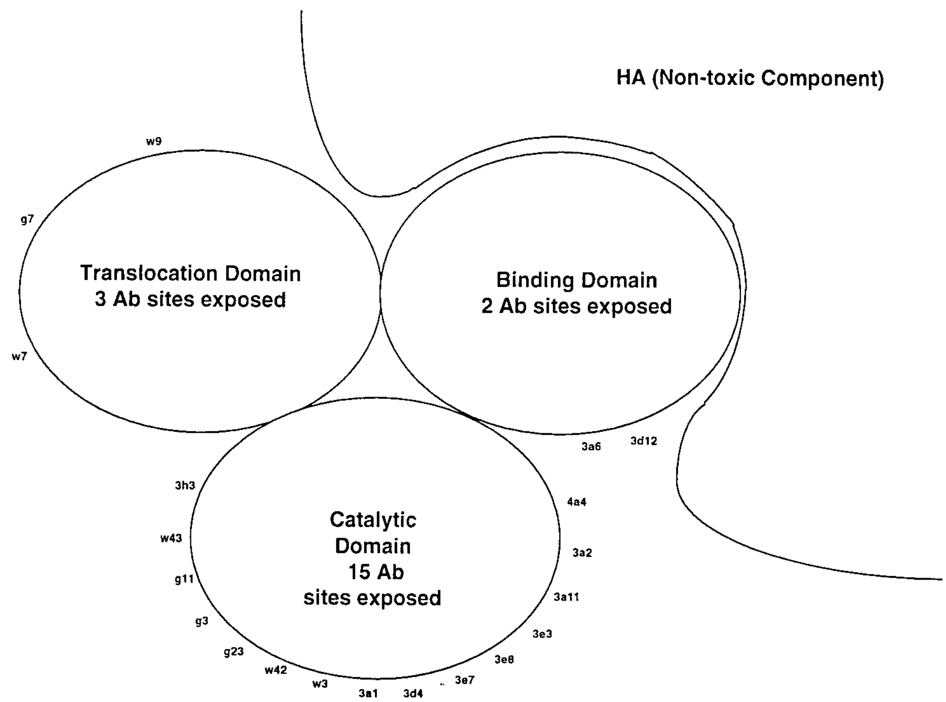

FIG. 3. Representation of a possible arrangement of BT with respect to HA. Only clones which bind the HA-BT complex are shown. The binding and translocation domains are covered partially by HA. Ab, antibody.

exposed or hidden epitopes in the BT and in the HA-BT complex. All of the antibodies specific to the translocation domain also recognized the HA-BT, indicating that the translocation domain is as exposed to the solvent in the complex (Fig. 3) as in the holotoxin (Table 1).

Not all of the scFv which bound the individual domains bound the BT holotoxin. Twenty-two of the 26 antibodies that recognized binding domain also recognized the BT. Thus, 4 antibody sites on the binding domain are covered by the catalytic or translocation domain in the BT (Table 1). However, not all of these scFv bound when the BT was complexed with the HA. Of the 22 exposed sites of binding domain on BT, only 2 bound the HA-BT complex. Therefore, the majority of antibodies to the binding domain recognize epitopes that must be covered by HA in the HA-BT complex (Fig. 3).

Fifteen antibodies were deduced to bind the catalytic domain. These antibodies were inferred by subtracting the antibodies that bound the binding and translocation domains from the antibodies that bound BT, since it is assumed that all of the antibodies must bind a domain of BT. All of these 15 antibodies bind an epitope that is accessible in the HA-BT complex. These 15 antibodies may bind conformational epitopes shared between domains. Such epitopes may not exist in the separate domains.

The model illustrated in Fig. 3 is subject to several caveats. Since the sequences of the epitopes are unknown, it is not possible to know the distribution of antibody binding sites. Hence the epitopes could be distributed evenly on the exposed surfaces or could be concentrated in certain regions of the protein. If the epitopes are clustered together, the area of BT covered by HA may be overestimated. If the epitopes are spaced regularly, the area of BT covered by HA may be underestimated. In either case, verification requires mapping of these antibodies to specific sequences of BT. Finally, since the model is drawn in two dimensions, it may not depict accurately the surface area of BT covered by HA. In addition, the arrangement of exposed and unexposed epitopes may be different from that diagrammed. The representation shows contiguous groups of exposed or unexposed epitopes that may be commingled.

The recombination experiments were performed to determine whether purified BT would interact with purified HA to reform the stable HA-BT complex at physiological pH. Since HA was undetectable by any of the antibody clones, the clones that bound to recombined HA-BT must bind exposed regions of BT. If no reconstitution of the complex occurred, recombined HA-BT should show the same number of clones as purified BT. If the HA-BT complex was formed, then recombined HA-BT should exhibit a positive reaction with the same clones as the purified HA-BT complex. The results from Table 1 indicate that an incomplete recombination took place. Whereas 40 clones recognized BT and 20 clones recognized the HA-BT complex, 37 clones bound recombined HA-BT. The three clones found in recombined HA-BT but not in the BT complex (s25, 2e6, and 2b6) are specific to the binding domain. Thus, under the recombination conditions, BT and HA do not fully reassemble. Some of the binding domain is left uncovered by HA.

Surprisingly, all of the epitopes that were covered in the HA-BT complex were mapped to the binding domain, strongly suggesting that the interactions between HA and BT are mediated by the binding domain. This idea is biologically relevant, since uncomplexed BT is susceptible to trypsin cleavage at the binding domain (22). Furthermore, the trypsinized BT could not bind to brain synaptosomes. When uncomplexed BT was incubated with trypsin, the translocation and catalytic domains showed no sign of proteolysis. Therefore, in the HA-BT complex, the HA may protect the binding domain of BT from proteolytic attack. These observations may guide in developing

antibodies for therapeutic design of neutralizing antibodies against botulism poisoning.

ACKNOWLEDGMENTS

We thank Bill Tepp and Bibhuti DasGupta, Department of Food Microbiology and Toxicology, University of Wisconsin, Madison, for generous supplies of BT and HA-BT complex. Also, we thank Birgitte Andersen for a careful reading of the manuscript.

We gratefully appreciate the support of U.S. Department of Army contracts DAMD17-93-C-3118 and DAMD17-94-C-4034.

REFERENCES

1. **Amersdorfer, P., et al.** Unpublished data.

1a. **Blasl, J., E. R. Chapman, E. Link, T. Binz, S. Yamasaki, P. De Camill, T. C. Südhof, H. Niemann, and R. Jahn.** 1993. Botulinum neurotoxin A selectively cleaves the synaptic protein SNAP-25. Nature **365:**160–163.

2. **Blauestein, R. O., W. J. Germann, A. Finklestein, and B. R. DasGupta.** 1987. The N-terminal half of the heavy chain of botulinum type A neurotoxin forms channels in planar phospholipid bilayers. FEBS Lett. **226:**115–120.

3. **DasGupta, B. R., and D. A. Boroff.** 1968. Separation of toxin and hemagglutinin from crystalline toxin of *Clostridium botulinum* type A by anion exchange chromatography and determination of their dimensions by gel filtration. J. Biol. Chem. **243:**1065–1072.

4. **DasGupta, B. R., D. A. Boroff, and E. Rothstein.** 1966. Chromatographic fractionation of the crystalline toxin of *Clostridium botulinum* type A. Biochem. Biophys. Res. Commun. **22:**750–756.

5. **DasGupta, B. R., and V. Sathyamoorthy.** 1984. Purification and amino acid composition of type A botulinum neurotoxin. Toxicon **22:**415–424.

6. **De Bellis, D., and I. Schwartz.** 1990. Regulated expression of foreign genes fused to lac: control by glucose levels in growth medium. Nucleic Acids Res. **18:**1311.

7. **Ekong, T. A. N., K. McLellan, and D. Sesardic.** 1995. Immunological detection of *Clostridium botulinum* toxin type A in therapeutic preparations. J. Immunol. Methods **180:**181–191.

8. **Fling, S. P., and D. S. Gregerson.** 1986. Peptide and protein molecular weight determination by electrophoresis using a high-molarity Tris buffer system without urea. Anal. Biochem. **155:**83–88.

9. **Hayashi, T., H. McMahon, S. Yamasaki, T. Binz, Y. Hata, T. C. Südhof, and H. Niemann.** 1994. Synaptic vesicle membrane fusion complex: action of clostridial neurotoxins on assembly. EMBO J. **13:**5051–5061.

10. **Hoogenboom, H. R.** 1991. Multisubunit proteins on the surface of filamentous phage: methodologies for displaying antibody (Fab) heavy and light chains. Nucleic Acids Res. **19:**4133–4137.

11. **Knox, J. N., W. P. Brown, and L. Spero.** 1970. The role of sulfhydryl groups in the activity of type A botulinum toxin. Biochim. Biophys. Acta **214:**350–354.

12. **Kozaki, S., Y. Kamata, T. Nagai, J. Ogasawara, and G. Sakaguchi.** 1986. The use of monoclonal antibodies to analyze the structure of *Clostridium botulinum* type E derivative toxin. Infect. Immun. **52:**786–791.

13. **Kozaki, S., A. Miki, Y. Kamata, T. Nagai, J. Ogasawara, and G. Sakaguchi.** 1989. Immunological characterization of papain-induced fragments of *Clostridium botulinum* type A neurotoxin and interaction of the fragments with brain synaptosomes. Infect. Immun. **57:**2634–2639.

14. **Kozaki, S., S. Nakaue, and Y. Kamata.** 1995. Immunological characterization of the neurotoxin produced by *Clostridium botulinum* type A associated with infant botulism in Japan. Microbiol. Immunol. **39:**767–774.

14a. **Lacy, B.** Unpublished data.

15. **Lamanna, C.** 1948. Hemagglutination by botulinal toxin. Proc. Soc. Exp. Biol. Med. **69:**332–336.

16. **Marks, J. D., H. R. Hoogenboom, T. P. Bonnert, J. McCafferty, A. D. Griffiths, and G. Winter.** 1991. By-passing immunization. Human antibodies from V-gene libraries displayed on phage. J. Mol. Biol. **222:**581–597.

17. **Munro, S., and H. R. Pelham.** 1986. An HSP70-like protein in the ER: identity with the 78 KDa glucose-regulated protein and immunoglobulin heavy chain binding protein. Cell **46:**291–300.

18. **Sathyamoorthy, V., B. R. DasGupta, J. Foley, and R. L. Niece.** 1988. Botulinum neurotoxin type A: cleavage of the heavy and light chains into two halves and their partial sequences. Arch. Biochem. Biophys. **266:**142–151.

19. **Sathyamoorthy, V., B. R. DasGupta, and R. L. Niece.** 1986. Botulinum neurotoxin type A, cleavage and partial sequence of the H chain. Fed. Proc. **45:**1793.

20. **Schier, R., R. F. Balint, A. McCall, G. Apell, J. W. Larrick, and J. D. Marks.** 1996. Identification of functional and structural amino-acid residues by parsimonious mutagenesis. Gene **169:**147–155.

21. **Schier, R., J. Bye, G. Apell, A. McCall, G. P. Adams, M. Malmquist, L. M. Weiner, and J. D. Marks.** 1996. Isolation of high-affinity monomeric human anti-c-erbB-2 single chain Fv using affinity-driven selection. J. Mol. Biol. **255:**28–43.

21a. **Sheets, M.** Unpublished data.

22. **Shone, C. C., P. Hambleton, and J. Melling.** 1985. Inactivation of Clostridium botulinum type A neurotoxin by trypsin and purification of two tryptic fragments. Eur. J. Biochem. **151:**75–82.

23. **Simpson, L. L.** 1980. Kinetic studies on the interaction between botulinum toxin type A and the cholinergic neuromuscular junction. J. Pharmacol. Exp. Ther. **212:**16–21.

24. **Sugii, S., I. Ohishi, and G. Sakaguchi.** 1977. Correlation between oral toxicity and in vitro stability of *Clostridium botulinum* type A and B toxins of different molecular sizes. Infect. Immun. **16:**910–914.

25. **Sugii, S., I. Ohishi, and G. Sakaguchi.** 1977. Intestinal absorption of botulinum toxins of different molecular sizes in rats. Infect. Immun. **17:**491–496.

26. **Sugiyama, H.** 1980. *Clostridium botulinum* neurotoxin. Microbiol. Rev. **44:**419–448.

27. **Sugiyama, H., I. Ohishi, and B. R. DasGupta.** 1974. Evaluation of type A botulinal toxin assays that use antitoxin to crystalline toxin. Appl. Microbio. **27:**333–336.

28. **Wong, C., et al.** Unpublished data.

Editor: A. O'Brien